Semiclassical theory of plate vibrations

E. Bogomolny and E. Hugues
Division de Physique Théorique*,
Institut de Physique Nucléaire,
91406 Orsay Cedex, France

November 1996

Abstract

We study semiclassically the biharmonic equation of flexural vibrations of elastic plates by a method which can easily be generalized for other models of wave propagation. The surface and perimeter terms of the asymptotic number of levels are derived exactly. The next constant term is also derived. A semiclassical approximation of the quantization condition is obtained, which, compared to the one for the membrane problem, contains an additional phase factor due to the shifts in phase waves get while reflecting from the boundary. A Berry-Tabor formula and a Gutzwiller trace formula are deduced for the integrable and chaotic cases respectively. From 600 eigenvalues of a clamped stadium plate, obtained by a specially developed numerical algorithm, the trace formula is assessed, looking at its Fourier transform compared with the membrane case. Extra peaks occur for a free plate, due to the existence of boundary modes.

IPNO/TH 96-46 (1996)

*Unité de Recherche des Universités Paris XI et Paris VI associée au C.N.R.S

1 Introduction

The semiclassical approximation via the Gutzwiller trace formula [1] is now one of the cornerstones of the modern approach to complicated quantum mechanical problems (see e.g. [2]). The driving ideas behind this method are very transparent and physically appealing. In the high-frequency limit, quantum particles have to propagate according to the rules of classical mechanics (with unavoidable complications near singular points and points of reflection). The main difference with classical mechanics comes from the fact that due to the linear character of the Schrödinger equation one has to sum over all possible classical paths. In particular, the Green function $G(\vec{r}_i, \vec{r}_f)$ of a n-dimensional quantum problem at the leading order of the semiclassical approximation can be written as the sum over all classical trajectories connecting the initial point $\vec{r}_i$ to the final point $\vec{r}_f$:

$$G(\vec{r}_i, \vec{r}_f) = \sum_{tr} A_{tr} e^{\frac{i}{\hbar} S_{tr}(\vec{r}_i, \vec{r}_f) - i\frac{\pi}{2}\nu_{tr}}. \tag{1}$$

Here $S_{tr}(\vec{r}_i, \vec{r}_f)$ is the classical action calculated along a given trajectory, A_{tr} is connected with the current conservation in the vicinity of this trajectory:

$$A_{tr} = \frac{1}{i\hbar(2\pi i\hbar)^{1/2}} \left| \det \frac{\partial^2 S_{tr}}{\partial \vec{r}_i^{\perp} \partial \vec{r}_f^{\perp}} \right|^{1/2}, \tag{2}$$

where $\vec{r}^{\perp}$ denotes the coordinates perpendicular to the trajectory and ν_{tr} is the Maslov index which counts the points along the trajectory at which the semiclassical approximation cannot be applied.

But all these arguments are not specific to quantum-mechanical problems. Equally well they can be applied to any phenomena of wave propagation when the wavelength λ is small compared to the characteristic dimensions of a system. The first problem which comes into mind is the propagation of high-frequency waves in elastic media. This is one of the oldest wave problems and it is the subject of many textbooks (see e.g. [3]-[6]). Acoustics, aeronautics, seismology are just a few examples of fields where high-frequency elastic waves are important. Recent laboratory experiments of vibrational spectra of simple geometrical objects [7, 8] and numerical calculations of high-frequency plate vibrations [9] strongly require the development of semiclassical theory of high frequency elastic waves. However, the recent tools and methods thoroughly investigated in the context of quantum chaos have not been (widely) applied to the general case. The first attempts [10, 11] have concentrated only on problems with ray splitting, when waves hitting a boundary give birth to multiple reflected and/or transmitted waves.

In this paper we shall focus on one of the simplest elastic problems, namely on the Kirchhoff model of transverse vibrations of two dimensional plates (see e.g. [4]). Derived from three dimensional elasticity, it describes the first flexural modes of a thin plate in the regime where the ratio of the thickness to the wavelength is relatively small. In a forthcoming paper about plate experiments [12], we will consider the different kinds of plate modes.

Let us consider a plate of thickness h, having its undeflected mid-surface $\mathcal{D}$ in the (x, y) plane, whose contour is $\mathcal{C}$. The main hypothesis of the classical plate theory is the conjecture that lines normal to the mid-surface stay undeformed and normal when the plate moves. The main effects neglected are the shear, which makes the direction of the lines independent, and the rotary inertia in the moment balance equations. If a tension T per unit length of the frontier is applied in its plane, for small deformation, one obtains a biharmonic equation for the mid-surface transverse displacement $w(x, y)$ [3]-[6]:

$$\rho h \frac{\partial^2 w}{\partial t^2} = T \Delta w - D \Delta^2 w, \tag{3}$$

where $D = Eh^3/12(1-\nu^2)$ is the flexural rigidity. ρ is the mass density, E is the Young elastic modulus and ν is the Poisson coefficient, both characterizing the mechanical properties of the plate. When the tension dominates, or in the long wavelength regime, one gets the membrane model described by the well known wave equation

$$\rho h \frac{\partial^2 w}{\partial t^2} = T \Delta w. \tag{4}$$

On the opposite limit, when stiffness dominates, or in the short wavelength regime, we get the purely biharmonic equation for flexural modes, or Kirchhoff model

$$\rho h \frac{\partial^2 w}{\partial t^2} = -D \Delta^2 w, \tag{5}$$

This plate problem has multiple connections with the membrane one. A previous study of this model was made in [9].

The periodic solutions $w(\vec{r},t) = W(\vec{r})e^{i\omega t}$ have to verify in $\mathcal{D}$ the following spectral problem

$$\Delta^2 W - k^4 W = 0, \tag{6}$$

where the modulus k of the wavevector $\vec{k}$ obeys the following dispersion relation

$$k^4 = \frac{12\rho(1-\nu^2)}{Eh^2}\omega^2. \tag{7}$$

For the membrane, the spectral equation is just the Helmholtz equation

$$\Delta W + k_m^2 W = 0, \tag{8}$$

or quantum billiard problem, which has been extensively studied in the quantum chaos field (see e.g. [2]). Here, $k_m^2 = \rho h\omega^2/T$.

Two conditions at the boundary $\mathcal{C}$ are needed to uniquely define the solution of the fourth order equation (6). The standard following self-adjoint boundary conditions are used for

- a clamped edge

$$W = 0, \ \frac{\partial W}{\partial n} = 0, \tag{9}$$

- a supported edge

$$W = 0, \ \Delta W - \nu' \frac{\partial^2 W}{\partial l^2} = 0, \tag{10}$$

- a free edge

$$\frac{\partial \Delta W}{\partial n} + \nu' \frac{\partial^3 W}{\partial l^2 \partial n} = 0, \ \Delta W - \nu' \frac{\partial^2 W}{\partial l^2} = 0, \tag{11}$$

where $\nu' = (1-\nu)$, $\partial/\partial l$ and $\partial/\partial n$ denote respectively the tangent and normal derivatives at the frontier $\mathcal{C}$, the normal being oriented towards the exterior of the domain.

The main difference between the biharmonic plate equation (6) and the Helmholtz equation (8) is that the former can be factorized into the Helmholtz operator and the operator $(\Delta - k^2)$ giving rise to exponentially decaying and increasing waves, so the solution can be written as a sum of solutions of each operator. The addition of exponential waves is then the main new feature introduced in this model compared to the quantum billiard problem.

The purpose of this paper is to develop the semiclassical trace formula for the high-frequency vibrations of the plate which will express the density of vibrational spectrum through the classical periodic orbits in complete analogy with the Gutzwiller trace formula for quantum problems. We shall perform the discussions in such a manner that one can use them not only for this particular problem but also in many similar problems.

The plan of the paper is the following. In the high-frequency limit, the characteristic change of all functions has to be of the order of $1/k$. Therefore, at the leading order of the semiclassical parameter, the reflection from any smooth boundary has to be the same as from the straight line. Then, in Section 2 we discuss exact solutions of the wave equation near a straight boundary for different boundary conditions. These solutions will serve us as the building block for further investigation. The calculation of the smooth part of the level density is done in Section 3. Section 4 is devoted to the derivation of the periodic orbit contribution to the trace formula. The study of an integrable case -the disk- is done in Section 5. In Section 6, the chaotic case of the plate in the shape of the stadium is considered and the comparison with numerical data is performed. In Appendix A we discuss a certain convenient expression for the second term of the Weyl expansion of the smooth part of the level counting function, in Appendix B we present the calculation of the curvature contribution to the third term, and in Appendix C we describe the method used to find numerically the spectrum of the clamped plate problem.

2 Half-plane solutions of wave equation

We have mentioned in the Introduction that the main difference between the biharmonic equation of plate vibrations and the quantum billiard equation is the existence of additional exponential waves of the type $\exp(\pm\vec{k}\cdot\vec{r})$. As these waves are non-propagating it is clear from physical considerations that (i) they can exist only near the boundary of the plate and (ii) only the waves **decreasing** from the boundary are allowed. If these conditions are not fulfilled the density of vibrational energy blows up somewhere inside the plate. It seems that the first time this picture has been discussed on particular examples in [13]. These simple considerations show that the structure of eigenfunctions of biharmonic equation (6) is the following. Far from the boundaries a wave function is a sum over different propagating waves of the type $\exp(\pm i\vec{k}\cdot\vec{r})$ as for usual billiard problems. And only in a small layer with the width of the order of $1/k$ the existence of other types of waves is important. It means that when $k \to \infty$ the solutions of this vibrational problem can be viewed as those of the billiard (membrane) problem but with different boundary conditions.

Taking into account that in the high-frequency limit the characteristic length on which any function is changed has to be also of the order of $1/k$, one is led to the simple conclusion that, at the leading order of semiclassical approximation, the reflection from any smooth boundary has to be close to the reflection from the straight line boundary (see Fig. 1). But this latter problem is very simple, and solved below.

Let us choose the x-axis along the boundary, the perpendicular y-axis being oriented towards the interior of the plate. In accordance with the above-mentioned statement, that the only permitted exponential modes have to decay from the boundary the solutions of the biharmonic equation (6), with a momentum p along the boundary, must have one of the following two forms:

- If $k > |p|$
$$W_{k,p}(x,y) = e^{ipx}[e^{-iqy} + Ae^{iqy} + Be^{-Qy}], \tag{12}$$
where $q = \sqrt{k^2 - p^2} = k\sin\theta$, θ being the angle between the reflected wave and the x-axis, and $Q = \sqrt{k^2 + p^2}$.

- If $k < |p|$
$$W_{k,p}(x,y) = e^{ipx}[e^{-Ry} + Be^{-Qy}], \tag{13}$$
where $R = \sqrt{p^2 - k^2}$.

The first case corresponds to the continuous spectrum and the second one gives the discrete spectrum (if any).

The clamped boundary conditions (9) $W|_{y=0} = 0$ and $\partial W/\partial y|_{y=0} = 0$ give the following equations for A and B:

$$1 + A + B = 0, \;\; iq(-1 + A) - QB = 0,$$

whose solution is

$$A = -e^{i\phi_c(\theta)},\ B = -(1+A), \tag{14}$$

where

$$\phi_c(\theta) = -2\arctan\left[\frac{\sin\theta}{\sqrt{1+\cos^2\theta}}\right]. \tag{15}$$

For the supported edge

$$A = -1,\ B = 0. \tag{16}$$

And for the free edge

$$A = -e^{i\phi_f(\theta)},\ B = (1+A)\frac{1-\nu'\cos^2(\theta)}{1+\nu'\cos^2(\theta)}, \tag{17}$$

where

$$\phi_f(\theta) = -2\arctan\left[\frac{\sin\theta}{\sqrt{1+\cos^2\theta}}\left(\frac{1+\nu'\cos^2\theta}{1-\nu'\cos^2\theta}\right)^2\right]. \tag{18}$$

The behavior of the phase shifts (15) and (18) is shown on Fig. 2.

It is easy to verify that the discrete spectrum exists only in the free edge case. The solution, in the form (13), is for

$$k(p) = |p|\kappa(\nu'), \tag{19}$$

where

$$\kappa(\nu') = \left[\nu'(2-3\nu') + 2\nu'\sqrt{2\nu'^2 - 2\nu' + 1}\right]^{\frac{1}{4}}. \tag{20}$$

Then

$$B = (\kappa^2(\nu') - \nu')/(\kappa^2(\nu') + \nu').$$

This mode propagates along the boundary and is analogous to the Rayleigh surface waves (see e.g. [4]). For a finite system of perimeter L, boundary modes can be quantized semiclassically by the condition

$$p_n L = 2n\pi, \tag{21}$$

n being an integer.

3 Mean staircase function

3.1 Surface and perimeter terms

The self-adjoint problem described by the biharmonic equation

$$(\Delta^2 - k^4)W(\vec{r}) = 0, \tag{22}$$

for $\vec{r}$ in $\mathcal{D}$, with any of the boundary conditions (9)-(11) on $\mathcal{C}$, admits a discrete real spectrum $0 \le k_1 \le \ldots \le k_n \le \ldots$. The eigenfunctions $W_n(\vec{r})$ are normalized in such a manner that

$$\sum_{n=1}^{\infty} \overline{W}_n(\vec{r}\,')W_n(\vec{r}) = \delta(\vec{r} - \vec{r}\,'). \tag{23}$$

Let $N(k)$ be the number of levels less than k, the staircase function, and $\tilde{N}(k)$ its mean asymptotic value. The standard approach to the asymptotic evaluation of $\tilde{N}(k)$ (see [14]) employs the Green function, which obeys to

$$(\Delta_{\vec{r}}^2 - k^4)G(\vec{r}, \vec{r}\,'; k) = \delta(\vec{r} - \vec{r}\,') \tag{24}$$

in $\mathcal{D}$, and to the given boundary conditions on $\mathcal{C}$. As for quantum problems this Green function can be written as the sum over all eigenvalues

$$G(\vec{r}, \vec{r}\,'; k) = \sum_{n=1}^{\infty} \frac{\overline{W}_n(\vec{r}\,')W_n(\vec{r})}{k_n^4 - k^4 - i\varepsilon}, \tag{25}$$

where $\varepsilon \to 0^+$. The importance of this function follows from the fact that any measurable quantity can be expressed through it. In particular, the density of the vibrational spectrum defined by

$$\rho(k) = \sum_{n=1}^{\infty} \delta(k - k_n) \tag{26}$$

is connected to the Green function by the standard formula

$$\rho(k) = \frac{1}{\pi} \Im \int_{\mathcal{D}} d\vec{r}\, 4k^3 G(\vec{r}, \vec{r}; k). \tag{27}$$

As it is well known (see [14]), the starting point of the semiclassical approximation is the construction of the free Green function which obeys Eq. (24) in the whole plane (without imposing any boundary conditions)

$$G_0(\vec{r},\vec{r}\,';k) = \frac{1}{(2\pi)^2}\int \frac{e^{i\vec{p}(\vec{r}-\vec{r}\,')}}{p^4-k^4-i\varepsilon}d\vec{p}. \tag{28}$$

From it, the dominant contribution to the smooth density of states (27) (the first Weyl term) equals

$$\bar{\rho}_1(k) = 4k^3\int_{\mathcal{D}} d\vec{r}\int \frac{d\vec{p}}{(2\pi)^2}\delta(p^4-k^4) = \frac{S}{2\pi}k. \tag{29}$$

where S is the area of $\mathcal{D}$. Therefore at the leading order in k the density of vibrational spectrum is the same as for billiard problems. On the contrary, the next terms of the Weyl expansion may be different.

It was noted in [14] that the second term of the Weyl expansion, proportional to the perimeter L of the boundary C, can be explicitly calculated from the knowledge of wave functions near the straight line boundary. The main point here is that in a small vicinity of any smooth boundary the Green function has to be close to the Green function of the half-plane.

We compute the latter from the knowledge of the exact solutions near a straight boundary discussed in Section 2. We have

$$G^{\pm}(\vec{r},\vec{r}\,';k) = \sum_{k',p}\frac{\overline{W}_{k',p}(\vec{r}\,')W_{k',p}(\vec{r})}{k'^4-k^4\mp i\varepsilon}, \tag{30}$$

where the sum is taken over all eigenvalues of our problem. Due to the translational invariance of the half-plane problem, any eigenfunction can be written in the form

$$W_{k',p}(\vec{r}) = \frac{1}{\sqrt{2\pi}}e^{ipx}V_{k',p}(y), \tag{31}$$

where p is a continuous parameter and $V_{k',p}$ is an eigenfunction of the one dimensional problem

$$\hat{H}(p,\hat{q})V_{k',p}(y) = k'^4V_{k',p}(y) \tag{32}$$

obeying the required boundary conditions. $H(p,q) = (p^2+q^2)^2$ with $\hat{q} = -id/dx$. For our problem $V_{k',p}(y)$ has to be proportional to the expression in square brackets of Eqs. (12) and (13) for continuous and discrete spectrum respectively. The constant of proportionality is determined from the normalization (23). As for quantum mechanical problems, wave functions of the discrete spectrum can be normalized by the usual condition

$$\int_0^{+\infty} |V_{k',p}(y)|^2 dy = 1, \tag{33}$$

and eigenfunctions of the continuous spectrum should be chosen in such a way that each plane wave in its expansion has the current equal to $1/\sqrt{2\pi}$. From the definition

$$g\hat{H}f - \overline{\hat{H}}gf = \hat{q}(g\hat{J}f),$$

it follows that the current operator $\hat{J}$ satisfies

$$g\hat{J}f = g\hat{q}^3 f + \bar{\hat{q}}g\hat{q}^2 f + \overline{\hat{q}^2}g\hat{q}f + \overline{\hat{q}^3}gf + 2p^2(g\hat{q}f + \bar{\hat{q}}gf),$$

and $\exp(-iq'x)\hat{J}\exp(iq'x) = \partial H/\partial q|_{q'}$. Therefore the normalized eigenfunctions of the continuous spectrum can be written in the following form

$$V_{k',p}(y) = \frac{1}{\sqrt{2\pi|\partial H/\partial q|_{q'}}}[e^{-iq'y} + Ae^{iq'y} + Be^{-Q'y}], \tag{34}$$

where $k' > |p|$, $q' = \sqrt{k'^2 - p^2}$ and $Q' = \sqrt{k'^2 + p^2}$. The values of A and B for standard boundary conditions are given in (14),(16) and (17).

The discontinuity of the free Green function $\Delta G_0(\vec{r}, \vec{r}\,'; k) \equiv G_0^+(\vec{r}, \vec{r}\,'; k) - G_0^-(\vec{r}, \vec{r}\,'; k)$ is

$$\begin{aligned} \Delta G_0(\vec{r}, \vec{r}\,'; k) &= \frac{i}{2\pi}\int_{-\infty}^{+\infty} dp \int_{-\infty}^{+\infty} dq' e^{ip(x-x')+iq'(y-y')}\delta((p^2+q'^2)^2 - k^4) \\ &= \frac{i}{2\pi}\int_{-k}^{k} dp\, e^{ip(x-x')}\frac{1}{|\partial H/\partial q|_q}(e^{iq(y-y')} + e^{-iq(y-y')}), \end{aligned} \tag{35}$$

where $q = \sqrt{k^2 - p^2}$. Correspondingly, the discontinuity of the exact half-plane Green function has the form

$$\begin{aligned} \Delta G(\vec{r}, \vec{r}\,'; k) &= i\int_{-k}^{k} dp\, e^{ip(x-x')}\overline{V_{k,p}(y')}V_{k,p}(y) \\ &+ i\int_{-\infty}^{+\infty} dp\, e^{ip(x-x')}\sum_j \overline{V_{k_j}(y')}V_{k_j}(y)\delta(k_j^4(p) - k^4), \end{aligned} \tag{36}$$

the last term being the sum, if any, over all discrete eigenvalues $k_j(p)$.

The second term of the Weyl expansion is expressed through the discontinuity of the Green function by the usual formula [14]

$$\tilde{\rho}_2(k) = 4k^3 L \lim_{\alpha \to 0^+} \frac{1}{2\pi i} \int_0^{+\infty} (\Delta G(\vec{r}, \vec{r}; k) - \Delta G_0(\vec{r}, \vec{r}; k)) e^{-\alpha y} dy, \qquad (37)$$

where the factor $\exp(-\alpha y)$ has been introduced for convergence, as for the continuous spectrum the integral over y diverges. One has first to compute the difference of the two expressions in (37) and then to perform the limit $\alpha \to 0^+$. The calculations are straightforward and one gets

$$\int_0^{+\infty} (\Delta G(\vec{r}, \vec{r}; k) - \Delta G_0(\vec{r}, \vec{r}; k)) e^{-\alpha y} dy = \frac{i}{2\pi} \int_{-k}^{k} dp \, \frac{1}{|\partial H / \partial q|_q}$$
$$\left[\frac{1}{2iq}(\bar{A} - A) + \frac{\pi}{2}\delta(q)(\bar{A} + A) + \frac{2}{Q + iq}\bar{B} + \frac{2}{Q - iq}B + \frac{1}{2Q}|B|^2 \right]$$
$$+ i \int_{-\infty}^{+\infty} dp \sum_j \delta(k_j^4(p) - k^4) \qquad (38)$$

Substituting here the expressions for A and B for a given choice of the boundary conditions, one can obtain the corresponding second term of the Weyl expansion. For example, for the clamped edge (9) the result is

$$\tilde{\rho}_2(k) = 2kL \int_{-k}^{k} \frac{dp}{2\pi} f(k, p) - \frac{L}{4\pi}, \qquad (39)$$

where

$$f(k, p) = \frac{1}{2\pi} \left[\frac{-(Q^2 - q^2)}{qQ(Q^2 + q^2)} \right]. \qquad (40)$$

It is easy to verify that the expression in the square bracket is just $d\phi_c(k, p)/dk^2$ where $\phi_c(k, p)$, with $p = k \cos\theta$, is the phase shift due to the reflection on the clamped edge (see (15)). This is not a coincidence. In Appendix A, following [15], we will show that it is a consequence of the Krein formula [16]. The function $f(k, p)$ in general can be written in the form

$$f(k, p) = \frac{1}{2\pi} \frac{d}{dk^2} \text{Arg det } S(k, p) \qquad (41)$$

where S is the scattering matrix for a given problem. In our case the S matrix coincides with the coefficient $A = -\exp(i\phi(\theta))$ and the second term of the Weyl expansion for the smooth staircase function takes the form for any boundary conditions

$$\tilde{N}_2(k) = L\int_{-k}^{k}\frac{dp}{2\pi}(-\frac{1}{4}+\frac{1}{2\pi}\phi(k,p)) + L\int_{-\infty}^{+\infty}\frac{dp}{2\pi}n_{d.s.}(k,p). \qquad (42)$$

The first term comes from the δ-function singularity, the second is the contribution of continuous spectrum and the third one is the staircase function of pure discrete spectrum. As the functions $\phi(k,p)$ and $n_{d.s.}(k,p)$ are homogeneous functions one obtains

$$\tilde{N}_2(k) = \beta\frac{L}{4\pi}k, \qquad (43)$$

β being given by

$$\beta = -1 + 2\int_{-1}^{1} dt\ \frac{1}{2\pi}\phi(1,t) + 2\int_{-\infty}^{+\infty} dt\ n_{d.s.}(1,t). \qquad (44)$$

For the three standard boundary conditions (9)-(11) the value of this coefficient is the following

- The clamped edge

$$\beta_c = -1 - \frac{4}{\pi}\int_0^1 \arctan\left[\frac{\sqrt{1-t^2}}{\sqrt{1+t^2}}\right] dt = -1 - \frac{\Gamma(3/4)}{\sqrt{\pi}\Gamma(5/4)} \approx -1.76279 \qquad (45)$$

- The supported edge

$$\beta_s = -1. \qquad (46)$$

- The free edge

$$\beta_f(\nu) = -1 + 4\left[\nu'(2-3\nu') + 2\nu'\sqrt{2\nu'^2 - 2\nu' + 1}\right]^{-1/4} - \frac{4}{\pi}\int_0^1 \arctan\left[\frac{\sqrt{1-t^2}}{\sqrt{1+t^2}}\left(\frac{1+\nu' t^2}{1-\nu' t^2}\right)^2\right] dt. \qquad (47)$$

For the membrane with the Dirichlet boundary conditions $\beta = -1$.

All these results were rigorously demonstrated in [15]. We have presented the above derivation in order to stress that all steps are exactly the same as for usual membrane problems [14].

3.2 Constant terms

The next term of the Weyl expansion should be a constant c_0, as for membrane problems, sum of the contributions from the curvature and from the corners of the boundary, if they exist.

In Appendix B, we show that the curvature contribution, as in billiard problems (see [17]), has the form

$$c_0^a = \alpha^a \int_{C_a} \frac{dl}{R(l)} \tag{48}$$

for the condition a on the boundary part C_a, R being the curvature radius. For a clamped edge, we find $\alpha^c = 1/3\pi$.

The corner contributions require the knowledge of the exact solution of the biharmonic equation for the infinite wedge with the same boundary conditions, which is not known at the moment.

The exception is the contribution from the corners which appear after desymmetrization of the region with respect to discrete symmetry. In the current case of parity transformation $x \to -x$, the eigenfunction is either even ($\varepsilon = +1$) or odd ($\varepsilon = -1$). The above derivation can be done taking, in place of Eq. (31), the following form of eigenfunctions for a boundary condition a

$$W^a_{k',p}(\vec{r}) = \frac{1}{\sqrt{2\pi}}(e^{ipx} + \varepsilon e^{-ipx}) V^a_{k',p}(y). \tag{49}$$

After integration over x, one gets the additional term

$$\varepsilon \frac{1}{2\pi} \delta(p).$$

From Eq. (42), the contribution of these corners will be the following:

$$c_0^{((\varepsilon)-a)} = \frac{\varepsilon}{4}\left[-\frac{1}{4} + \frac{1}{2\pi}\phi(k,0)) + n_{d.s.}(k,0)\right]. \tag{50}$$

Then, for a clamped edge one gets

$$c_0^{((\varepsilon)-c)} = -\frac{\varepsilon}{8}, \tag{51}$$

for a supported edge

$$c_0^{((\varepsilon)-s)} = -\frac{\varepsilon}{16}, \tag{52}$$

which is the same result as for a right angle corner in the membrane case, and for a free edge

$$c_0^{((\epsilon)-f)} = \frac{\varepsilon}{8}. \tag{53}$$

4 Boundary integral equations

The standard method of deriving the trace formula for quantum billiards is the reduction of the problem to boundary integral equations [14]. These equations serve also as a starting point of many different approaches to semi-classical quan[25], [26].

We shall discuss in this section the construction of boundary equations for the biharmonic equation

$$(\Delta^2 - k^4)W(\vec{r}\,) = 0, \tag{54}$$

with self-adjoint boundary conditions.

Let us define the Green function of the following two free problems

$$(\Delta_{\vec{r}} + k^2)G^{(+)}(\vec{r}, \vec{r}\,'; k) = \delta(\vec{r} - \vec{r}\,'), \tag{55}$$

and

$$(\Delta_{\vec{r}} - k^2)G^{(-)}(\vec{r}, \vec{r}\,'; k) = \delta(\vec{r} - \vec{r}\,'). \tag{56}$$

These functions admit the usual integral representation

$$G^{(\pm)}(\vec{r}, \vec{r}\,'; k) = -\int \frac{d\vec{p}}{(2\pi)^2} \frac{e^{i\vec{p}\cdot(\vec{r}-\vec{r}\,')}}{p^2 \mp (k^2 + i\varepsilon)}, \tag{57}$$

and can be expressed through the Bessel functions as follows

$$G^{(+)}(\vec{r}, \vec{r}\,'; k) = \frac{1}{4i} H_0^{(1)}(k|\vec{r} - \vec{r}\,'|), \tag{58}$$

$$G^{(-)}(\vec{r}, \vec{r}\,'; k) = -\frac{1}{2\pi} K_0(k|\vec{r} - \vec{r}\,'|). \tag{59}$$

The reduction of 2-dim Green functions to 1-dim ones is also useful:

$$G^{(+)}(\vec{r}, \vec{0}; k) = \int \frac{dp}{2\pi} e^{ipx} \frac{e^{iq|y|}}{2iq}, \tag{60}$$

$$G^{(-)}(\vec{r},\vec{0};k) = -\int \frac{dp}{2\pi} e^{ipx} \frac{e^{-Q|y|}}{2Q}, \tag{61}$$

where $q = \sqrt{k^2 - p^2}$ and $Q = \sqrt{k^2 + p^2}$. In the following we will drop k in the notations for convenience.

We shall look for a solution of the biharmonic equation (54) in the form

$$W(\vec{r}) = \int_C G^{(+)}(\vec{r},\alpha)\mu(\alpha)d\alpha + \int_C G^{(-)}(\vec{r},\alpha)\nu(\alpha)d\alpha, \tag{62}$$

where α denotes a point on the boundary of the plate and the integration in (54) is taken over the whole boundary. The function W defined by this expression satisfies Eq. (54) with arbitrary functions μ and ν. There are many different forms of W with this property. As we shall consider below only formal semiclassical transformations and shall not discuss problems of convergence, all these forms are equivalent and Eq. (62) is the simplest. But in real calculations other forms are preferable.

To define functions μ and ν one has to impose the boundary conditions. We present here the derivation of the system of equations for μ and ν in the case of a clamped edge (9) where the function W and its normal derivative equal zero at an arbitrary point β on the boundary.

$$W(\beta) = 0, \quad \frac{\partial W}{\partial n_\beta}(\beta) = 0. \tag{63}$$

As any Green function has a logarithmic singularity when the difference of arguments is small

$$G^{\pm}(\vec{r},\vec{r}\,') \to \frac{1}{2\pi}\log|\vec{r}-\vec{r}\,'|,$$

a care should be taken when computing the boundary limit of its normal derivative. It is well known (see e.g. [27]) that

$$\lim_{x\to\beta}\int_C \frac{\partial G(x,\alpha)}{\partial n} f(\alpha)d\alpha = \frac{1}{2}f(\beta) + \int_C \frac{\partial G(\beta,\alpha)}{\partial n_\beta} f(\alpha)d\alpha. \tag{64}$$

The integration here is taken over a closed surface and n_β denotes the inward normal at point β. (The simplest way to check this relation is to consider the integral over a straight line.) Using this formula one gets the following system of equations to determine the functions μ and ν

$$\int_C G^{(+)}(\beta,\alpha)\mu(\alpha)d\alpha + \int_C G^{(-)}(\beta,\alpha)\nu(\alpha)d\alpha = 0, \tag{65}$$

$$\frac{1}{2}\mu(\beta) + \frac{1}{2}\nu(\beta) + \int_C \frac{\partial G^{(+)}(\beta,\alpha)}{\partial n_\beta}\mu(\alpha)d\alpha + \int_C \frac{\partial G^{(-)}(\beta,\alpha)}{\partial n_\beta}\nu(\alpha)d\alpha = 0. \quad (66)$$

To find the semiclassical limit $k \to \infty$ of these equations it is necessary to separate the contributions due to points at short distances from those due to points at large ones (see [25]).

Let us divide each integral in Eqs. (65) and (66) into two parts separating a small vicinity of the point β:

$$\int_C f(\beta,\alpha)d\alpha = \int_{\beta-\Delta}^{\beta+\Delta} f(\beta,\alpha)d\alpha + \int_{C_\Delta} f(\beta,\alpha)d\alpha, \quad (67)$$

where the second integral is taken over the rest of the boundary. Choosing Δ in such a way that $1/k \ll \Delta \ll l_0$ where l_0 is a characteristic scale of the boundary it is easy to demonstrate that

$$\int_{\beta-\Delta}^{\beta+\Delta} f(\beta,\alpha)d\alpha \stackrel{k\to\infty}{\to} \int_{-\infty}^{+\infty} f(\beta,\gamma)d\gamma, \quad (68)$$

where the last integral is taken over the straight (s.l.) line and the corrections could, in principle, be computed.

As $\partial G(\beta,\alpha)/\partial n_\beta$ equals zero on a straight line Eqs. (65) and (66) can be asymptotically rewritten in the following form

$$\int_{s.l.} G^{(+)}(\beta,\gamma)\mu(\gamma)d\gamma + \int_{C_\Delta} G^{(+)}(\beta,\alpha)\mu(\alpha)d\alpha +$$
$$\int_{s.l.} G^{(-)}(\beta,\gamma)\nu(\gamma)d\gamma + \int_{C_\Delta} G^{(-)}(\beta,\alpha)\nu(\alpha)d\alpha = 0, \quad (69)$$

$$\frac{1}{2}\mu(\beta)+\frac{1}{2}\nu(\beta)+\int_{C_\Delta} \frac{\partial G^{(+)}(\beta,\alpha)}{\partial n_\beta}\mu(\alpha)d\alpha+\int_{C_\Delta} \frac{\partial G^{(-)}(\beta,\alpha)}{\partial n_\beta}\nu(\alpha)d\alpha = 0. \quad (70)$$

Now it is convenient to consider the Fourier transformation of these equations. Let

$$\mu(\alpha) = \int \mu_p e^{ip\alpha}dp, \qquad \nu(\alpha) = \int \nu_p e^{ip\alpha}dp,$$
$$G^{(\pm)}(\beta,\alpha) = \int\int G^{(\pm)}_{p,p'} e^{ip\beta - ip'\alpha}dp dp'. \quad (71)$$

In the leading order of semiclassical approximation

$$\frac{\partial G^{(+)}(\beta,\alpha)}{\partial n_\beta} = -i\int\int qG^{(+)}_{p,p'}e^{ip\beta-ip'\alpha}dpdp' \tag{72}$$

$$\frac{\partial G^{(-)}(\beta,\alpha)}{\partial n_\beta} = \int\int QG^{(+)}_{p,p'}e^{ip\beta-ip'\alpha}dpdp'. \tag{73}$$

Taking into account these formulae and Eqs. (60) and (61) we find that μ_p and ν_p have to satisfy the following system of equations

$$(M_0\delta_{p,p'} + M_{p,p'})\begin{pmatrix}\mu_p\\ \nu_p\end{pmatrix} = 0, \tag{74}$$

where

$$M_0 = \frac{1}{2}\begin{pmatrix}-i/q & -1/Q\\ 1 & 1\end{pmatrix}, \tag{75}$$

$$M_{p,p'} = \begin{pmatrix}G^{(+)}_{p,p'} & G^{(-)}_{p,p'}\\ -iqG^{(+)}_{p,p'} & QG^{(-)}_{p,p'}\end{pmatrix}. \tag{76}$$

The condition of compatibility, the quantization condition, is the zero of the determinant

$$\det(M_0\delta_{p,p'} + M_{p,p'}) = 0, \tag{77}$$

which can be transformed to the form

$$\det(\delta_{p,p'} - T_{p,p'}) = 0, \tag{78}$$

where the total transfer matrix $T_{p,p'} = -2M_0^{-1}M_{p,p'}$ can be rewritten within semiclassical accuracy as

$$T_{p,p'} = -\begin{pmatrix}-2\frac{Q-iq}{Q+iq}(\frac{\partial G^{(+)}}{\partial n_\beta})_{p,p'} & \frac{4iq}{Q+iq}(\frac{\partial G^{(-)}}{\partial n_\beta})_{p,p'}\\ \frac{4Q}{Q+iq}(\frac{\partial G^{(+)}}{\partial n_\beta})_{p,p'} & 2i\frac{Q-iq}{Q+iq}(\frac{\partial G^{(-)}}{\partial n_\beta})_{p,p'}\end{pmatrix}. \tag{79}$$

When $k \to \infty$ with $|\alpha - \beta| > 0$

$$G^{(-)}(\beta,\alpha) \approx e^{-k|\beta-\alpha|} \to 0$$

and one can ignore all terms in $T_{p,p'}$ which contain $G^{(-)}$. Finally we get that in the leading order of semiclassical approximation the quantization condition can be written in the form very similar to the one for quantum billiard problem with the Dirichlet boundary conditions

$$\det(1 - 2e^{i\phi(p,k)}(\frac{\partial G^{(+)}}{\partial n_\beta})_{p,p'}) = 0, \tag{80}$$

where

$$e^{i\phi(p,k)} = \frac{Q - iq}{Q + iq}.$$

The only difference between this expression and that of quantum billiard is that for the latter $\phi(p,k) = 0$ (note that in the leading order $\partial G(\beta,\alpha)/\partial n_\beta = -\partial G(\beta,\alpha)/\partial n_\alpha$). This result is very satisfactory from semiclassical point of view. It is quite natural that the reflection from a smooth boundary should be close to the one from a straight line. Then, the only difference between these two problems is in the phase shift, or more generally, in the S matrix for the scattering from the straight line, whose calculation is usually quite simple (see Section 2). It is clear that the same conclusion can be derived for other boundary conditions.

Analogous considerations as in [14] permit also to obtain the semiclassical expression for the Green function as a sum over classical trajectories. The presence of the additional phase shift after each reflection from the boundary is the main difference between the plate vibration and the corresponding billiard problem.

4.1 The trace formula

The additional phase in Eq. (80) does not change any standard steps by which one comes from this determinant condition (80) to the Gutzwiller trace formula (see e.g. [25]). Using the formulae

$$N^{(osc)}(k) = \frac{1}{\pi}\Im \log\det(1 - T),$$

and

$$\log\det(1 - T) = tr\log(1 - T) = -\sum_{n=1}^{\infty}\frac{(-1)^{n+1}}{n}trT^n,$$

and computing all traces in the stationary phase approximation one obtains that the periodic orbits contribution for the transverse plate vibrations can be written in the following form

$$N^{(osc)}(k) = \frac{1}{\pi}\Im \sum_{ppo} \sum_{n=1}^{\infty} \frac{1}{|\det(M_p^n - 1)|^{1/2}} \exp\left[in(S_p - \frac{\pi}{2}\mu_p + \Phi_p)\right], \quad (81)$$

where the summation is taken over all primitive periodic orbits corresponding to classical motion with specular reflection at the boundary. S_p is the classical action along this trajectory: $S_p = kl_p$, where l_p is the length of a periodic orbit. M_p is the monodromy matrix of this periodic orbit. μ_p is the Maslov index of the billiard problem with the Dirichlet boundary conditions. The only unusual quantity here is the additional phase shift Φ_p due to the existence of exponentially decreasing waves in a small layer around the boundary. For clamped, supported, and free edges the values of this phase shift are given in Eqs. (9)-(11). For other boundary conditions it has to be determined from the scattering from the straight line boundary.

The total staircase function has the form

$$N(k) = \tilde{N}(k) + N^{(osc)}(k), \quad (82)$$

where $\tilde{N}(k)$ is the smooth part of the staircase function whose calculation has been discussed in Section 3.

4.2 The Fredholm equations

The boundary integral equations are a quite natural way of representing the spectral problem as a Fredholm integral equation. For quantum problems it has been done in [26]. To do it for the plate, it is convenient to use another representation of formal solutions of the biharmonic equation (54). The main drawback of the most simple one (62) is that the corresponding equations (65), (66) have not automatically the Fredholm form.

Let us represent our solution in the following form

$$W(\vec{r}) = \int_C \frac{\partial G^{(+)}}{\partial n_\alpha}(\vec{r}, \alpha)\mu(\alpha)d\alpha + \int_C G^{(-)}(\vec{r}, \alpha)\nu(\alpha)d\alpha, \quad (83)$$

with unknown functions μ and ν (different from the ones above). Using the fact that $\partial^2 G(\beta, \alpha)/\partial n_\beta \partial n_\alpha$ remains continuous on the boundary (see e.g.

[27]), one easily derives the following system of equations for the clamped edge boundary conditions

$$\psi_i(\beta) + \int_C K_{i,j}(\beta,\alpha)\psi_j(\alpha)d\alpha = 0, \tag{84}$$

where $i, j = 1, 2$ and

$$\psi(\beta) = \begin{pmatrix} \mu(\beta) \\ \nu(\beta) \end{pmatrix}. \tag{85}$$

The kernel $K_{i,j}$ has the form

$$K(\beta,\alpha) = 2\begin{pmatrix} -\frac{\partial G^{(+)}(\beta,\alpha)}{\partial n_\alpha} & -G^{(-)}(\beta,\alpha) \\ \frac{\partial^2 G^{(+)}(\beta,\alpha)}{\partial n_\beta \partial n_\alpha} & \frac{\partial G^{(-)}(\beta,\alpha)}{\partial n_\beta} \end{pmatrix}. \tag{86}$$

These equations have exactly the Fredholm form with (slightly singular) kernel, and the compatibility equation (the zeta function of this problem) has the form of the Fredholm determinant

$$\det(1 + K) = 0. \tag{87}$$

Therefore all consequences of the Fredholm theory (see [27], [26]) can be applied for vibrational problems as well.

5 The disk shaped plate

In this Section, we will study the particular case of an integrable system, the disk plate. The advantage is that knowing exactly the classical and the wave solutions, we can easily check the validity of the semiclassical formulae.

In polar coordinates (r, θ) relative to the center of the disk of radius R, this problem is separable, and due to the factorization property, and to the fact that the solution must be finite at the center, one finds the following form of eigenfunctions

$$W(r,\theta) = [aJ_m(kr) + bI_m(kr)][A\cos(m\theta) + B\sin(m\theta)], \tag{88}$$

for any integer $m \geq 0$. J_m and I_m are the Bessel functions of the first kind and the hyperbolic one. The boundary conditions at $r = R$ give a system of two linear equations in the unknown coefficients a and b, which has non trivial solution if and only if the determinant of the coefficients vanishes. If we call $x = kR$, we have the following quantization relations for k for the boundary conditions we will study below :

- the clamped edge

$$J_m(x)I_m'(x) - J_m'(x)I_m(x) = 0, \tag{89}$$

- the free edge

$$\frac{x^3J_m'(x) + m^2\nu'[xJ_m'(x) - J_m(x)]}{x^3I_m'(x) - m^2\nu'[xI_m'(x) - I_m(x)]} = \frac{x^2J_m(x) + \nu'[xJ_m'(x) - m^2J_m(x)]}{x^2I_m(x) - \nu'[xI_m'(x) - m^2I_m(x)]}. \tag{90}$$

These relations have an infinite number of positive eigenvalues $k_{m,1} < \ldots < k_{m,n} < \ldots$. As can be seen from (88), they are doubly degenerate for $m > 0$.

In the following subsections, we will study the mean staircase function, the periodic orbit sum formula describing the fluctuations around this mean behavior, and the statistics of the spectra for the clamped and free boundary conditions.

5.1 Mean staircase function

In Section 3, the first three terms of the staircase function were derived. As for quantum billiards, we conjecture here the following expansion when $k \to +\infty$

$$\tilde{N}(k) = \frac{S}{4\pi}k^2 + \beta\frac{L}{4\pi}k + c_0 + c_{-1}\frac{1}{k} + o(\frac{1}{k}). \tag{91}$$

The clamped plate

We have determined the spectra for $k \leq 400$ for a unit radius disk (39641 eigenvalues). On Fig. 3 we have plotted the difference between the staircase function and its mean taking only the surface and perimeter terms, which confirms that it oscillates around a constant. The amplitude of the oscillations attains as high values as 20, which is characteristic of an integrable system. In order to determine the constant term, we integrate this function, which should give $c_0k + c_{-1}\log k$ as mean behavior, the amplitude of the oscillations being small in comparison[1]. Fitting this curve, we see that the conjecture seems valid. For the complete disk, the constant, which is only a curvature effect, is $c_0^c = 2/3 \pm 10^{-5}$, which gives $\alpha^c = 1/3\pi \pm 2 \cdot 10^{-6}$ in Eq. (48), in accordance with the exact calculation (see Eq. (155)) done in Appendix B. Using the half and quarter of the disk, with odd symmetry on the straight edges (supported edges), we introduce corner terms. We find numerically the values predicted by Eqs. (51) and (52), to an error of $5 \cdot 10^{-4}$.

The free plate

The spectra has been also determined for $k \leq 400$ for different values of ν from 0 to 0.5 (40368 eigenvalues in this last case). Due to the order, at least 2, of the boundary conditions, supplementary solutions, not in the form of (88) appear: these are the constant, and the two independant linear solutions in the cartesian coordinates. The modes of the discrete spectrum, discussed in Section 2, verify here semiclassically $k_{m,1} < m$, and special attention is needed to find them. On the oscillatory part of the staircase function (Fig. 4), it can be checked, for $\nu = 0.5$ ($\beta_f(0.5) \approx 1.8871194$), that there is no missing eigenvalues. For the complete disk, the constant term due to curvature is found to be $c_0^f = 2/3 + 1.1 \cdot 10^{-4} \pm 4 \cdot 10^{-5}$ for $0 \leq \nu \leq 0.5$, which is very close from the clamped result. The ν dependence of this contribution, if it exists as is expected, is then inside the error bar. Using the half and quarter of the disk as in the clamped case, we also find numerically the value predicted by Eq. (53), to an error of $6 \cdot 10^{-5}$.

5.2 Oscillatory part of the density of states

When the system is integrable, we know that the density of states

$$\rho(k) = \sum_{m=-\infty}^{+\infty} \sum_{n=1}^{+\infty} \delta(k - k_{m,n}) \tag{92}$$

can be expressed at high energy, via the Poisson summation formula and stationary phase approximation, by a sum over periodic orbits at the leading

[1]The dominant oscillation term $k^r \sum_p A_p \sin(kl_p + \psi_p)$, due to periodic orbits, has been shown to be smaller than the perimeter term linear in k, so the integration, giving the dominant term $k^r \sum_p \frac{A_p}{l_p} \cos(kl_p + \psi_p)$ is less than $c_0 k$.

order, as was first derived by Berry and Tabor [18]-[19]. But, as was shown in Section 4, (80) is applicable for any system, leading semiclassically to a sum over periodic orbits whose coefficients depend on their properties, in particular their stability and the fact that they appear alone or in families (here, because of the rotation symmetry, all periodic orbits appear in continuous families). Furthermore, (80) differs from the Dirichlet membrane result only by the presence of the phase factor $\exp(i\phi(p,k))$. Then, the periodic orbit sum for the plate is the same as for the membrane (see e.g. [23]). provided that one adds the supplementary phase for clamping. At the semiclassical level, the oscillatory part of the density of states follows

$$\rho^{(osc)}(k) = \sum_{m=1}^{+\infty} \sum_{n=2m}^{+\infty} a_{m,n}(k) \cos(kl_{m,n} + \psi_{m,n}). \tag{93}$$

The sum is made over all the periodic orbits (m,n) of the disk. m being the winding number and n the number of bounces on the frontier. $l_{m,n} = 2n\sin(\pi m/n)$ is the length of the orbit,

$$a_{m,n}(k) = g_{m,n}\sqrt{\frac{4k}{\pi n}\sin^3(\frac{\pi m}{n})},$$

$g_{m,n}$ is 1 for the bouncing ball orbits $(n = 2m)$ and otherwise 2. The periodic orbit makes an angle $\theta_{m,n}$ with the frontier, and the phase is expressed by

$$\psi_{m,n} = n[\phi(\theta_{m,n}) + \frac{\pi}{2}] + \frac{\pi}{4}, \tag{94}$$

where ϕ is the additional phase shift given by (15) or (18) for clamped and free boundary conditions respectively. The $k^{1/2}$ dependence of the coefficients is due the fact that periodic orbits appear in continuous families. For a fixed winding number m, $l_{m,n}$ grows from $l_{m,2m} = 4m$ for the bouncing ball orbit to $l_{m,\infty} = 2\pi m$ for the whispering gallery orbits.

In order to look at the precision of this semiclassical formula, a Gaussian-weighted Fourier transform

$$F[\rho](l) = 4\sqrt{\frac{\beta}{\pi}} \int_0^{k_{max}} \frac{e^{-\beta k^2}}{k^r} e^{-ikl} \rho(k) dk \tag{95}$$

is performed, where r is the power dependence in k of the semiclassical coefficients in the periodic orbit sum formula. As $k_{max} \to \infty$, and for

$$\rho^{(osc)}(k) = k^r \sum_{p.o.p} A_p \cos(kl_p + \psi_p), \tag{96}$$

one gets for $l > 0$

$$F[\rho^{(osc)}](l) \approx \sum_{p.o.p} A_p e^{i\psi_p} \left[e^{\frac{-(l-l_p)^2}{4\beta}} + ig(\frac{l-l_p}{2\sqrt{\beta}}) \right], \tag{97}$$

where g is an odd function smaller than the Gaussian. The Fourier transform should then give peaks at periodic orbit lengths l_p, with amplitude $A_p \exp(i\psi_p)$. β is chosen to have $\exp(-\beta k_{max}^2)$ sufficiently small (typical value of 0.01) to get the thinnest peaks with the lowest spurious oscillations. When periodic orbit lengths differ by less than about $\sqrt{\beta}$, different peaks interfere, modifying shapes and amplitudes.

The clamped plate

On Fig. 5 is plotted the real part of $e^{-i\Psi_p} F[\rho]$, in the region of length around l_p. The Gaussian shape and amplitude of the peaks show that the semiclassical phase and amplitude are quite precise. All orbits of winding number 1 are visible, and as known for the quantum billiard case, the agreement decrease as the whispering gallery is attained, due to the fact that for modes confined near the boundary, the first semiclassical term becomes insufficient.

The free plate

In this case, boundary modes obey semiclassically, following Eqs (19)-(21)

$$k_n = \frac{2n\pi}{L}\kappa(\nu') \tag{98}$$

and should then give regularly spaced peaks in the Fourier transform at lengths $L_p = pL/\kappa(\nu')$. To see them clearly, and to minimize interference effects with periodic orbits peaks located on the left (mainly whispering gallery orbits of lengths just below pL), we choose $\nu = 0.5$ for which $\kappa(\nu') = 0.9891$ is the minimum. But this value remains quite close to 1 and the exponent of the first term in (13) $R = p\sqrt{1-\kappa^2(\nu')}$ is small for the considered interval of k. It prevents of using the standard asymptotics of the Bessel function and the semiclassical asymptotics for this particular eigenvalue is reached quite slowly. These peaks appear then smeared on a quite long distance on their left, as shown on Fig. 6. Here, the modes $k_{m,1}$ have been separated from the rest of the spectrum, and separate Fourier transforms show clearly the influence of this peak, located at $l = L_1 = 6.3524$. In the following, the first thousand eigenvalues are ignored to be closer to the semiclassical result.

Apart from this fact, the periodic orbit sum contains the same orbits and amplitudes for the membrane and for the plates, their classical limit being the same, and so no difference should be seen in $|F[\rho]|^2$ for these different cases for isolated peaks. On Fig. 7, a very good agreement is found between the three cases, except for the peak located at $l = 12$. Here, an exact degeneracy in orbit lengths occurs for the first time, corresponding to two times the hexagon orbit and three times the bouncing ball orbit. Semiclassically, the two associated terms have the same k dependence, but a different phase. Adding these two terms results in an amplitude $A^2_{m,D} = 0.0531$ for the Dirichlet membrane, $A^2_{p,c} = 0.1102$ for the clamped plate and $A^2_{p,f} = 0.4452$ for the free one. The agreement is rather good (see Fig. 7 (b)), taking account of all possible interferences between peaks.

5.3 Statistics of spectra

Integrable systems of the membrane type are known to have Poissonian statistics of energy levels ([18]). The same behavior is found for the disk[2] plates as is shown here on Fig. 8 for the nearest neighbor spacing distribution .

The second moment of the statistics of the staircase fluctuations,

$$< \delta^2 > (k) = \int_0^{k^2} [N(k') - \tilde{N}(k')]^2 dk'^2, \tag{99}$$

is shown to be proportional to Ck as $k \to \infty$ for two-dimensional integrable quantum billiards (see e.g. [20] and references therein), or proportional to $C'\sqrt{N}$. The same behavior is also found here for the disk plates as shown on Fig. 9.

6 The stadium shaped plate

In this Section we check numerically the semiclassical trace formula for systems whose classical limit is chaotic, and more precisely in the case where all periodic orbits are isolated or unstable. We will concentrate here on the

[2] In order to see a generic behavior, we have taken the half-disk, with odd symmetry to get rid of degeneracies.

stadium shape (a square glued with two half-disks), which has been proven to be ergodic [21], and which is today certainly the most studied non integrable quantum billiard. All its periodic orbits are unstable, except for the neutral bouncing ball orbits between the two straight lines.

We will be interested here in the spectra of odd-odd modes relatively to the two symmetry axes, which is equivalent to take the fourth of the stadium with supported boundary conditions on its symmetry lines. We obtained numerically (see Appendix C) the first 585 levels, corresponding to $k \leq 100$ for a surface equal to $\pi/4$ (circle radius $R = 1/\sqrt{1+4/\pi}$).

6.1 Mean staircase function

The perimeter term of the semiclassical expansion of the staircase function is obtained by summing over the contributions of each part of the boundary, that is, if we assume the same form (91) of the mean staircase function as for the disk

$$\bar{N}(k) = \frac{1}{16}k^2 + \frac{[(1+\pi/2)\beta_c + 3\beta_s]R}{4\pi}k + c_0 + c_{-1}\frac{1}{k} + o(\frac{1}{k}), \quad (100)$$

where the perimeter coefficient is $c_1 = -0.397521$. The constant term should have the same contributions as those of the quarter of a clamped disk studied in Section 5.1, that is $c_0 = 23/48$.

As the numerical data in this case is less precise than in the disk case, we fit the perimeter and constant coefficients. For better precision, we subtract first the oscillating contribution of the family of neutral orbits (see discussion below), which has a greater amplitude than the constant term. We find $c_1 = -0.39730 \pm 4.\ 10^{-5}$, and $c_0 = 23/48 \pm 4.\ 10^{-3}$, which is in very good agreement with predictions. Subtracting the two first terms to the staircase function (see Fig. 10), one gets oscillations whose amplitude is limited to a few unities, indicating a rigid spectrum, as in the membrane case.

6.2 Neutral orbits

The stadium billiard possesses bouncing ball orbits between the two straight lines of the square. They constitute a continuous family of neutral orbits, whose contribution differ from the isolated unstable orbits contribution obtained Section 4.1, and whose more careful derivation is done below.

Let us consider an infinite plate along the x-axis, whose width is $2b$, with clamped boundary conditions. Due to the symmetry with respect to the central line ($y = 0$) eigenfunctions of this problem can be classified by their parity. Writing the (odd) eigenfunctions as the corresponding sum of 4 different exponents

$$W_{k,p}(x, y) = e^{ipx}(\sin(qy) + B\sinh(Qy)), \tag{101}$$

where $p = k\cos\theta$, $q = \sqrt{k^2 - p^2} = k\sin\theta$, $Q = \sqrt{k^2 + p^2}$ and imposing clamped boundary conditions at the line $y = b$ one obtains the following quantization condition

$$Q\sin(qb)\cosh(Qb) - q\cos(qb)\sinh(Qb) = 0. \tag{102}$$

In the semiclassical limit ($k \to +\infty$), an implicit relation for $q(p, n)$ can be written neglecting exponentially small terms :

$$qb = \arctan\left[\frac{q}{\sqrt{2p^2 + q^2}}\right] + n\pi \tag{103}$$

where n is a positive integer. If we search the contribution to the density of states of such solutions for a strip of length a, we have to compute

$$\rho_b(k) = \frac{a}{2\pi}\int_{-\infty}^{+\infty} dp \sum_{n=1}^{+\infty} 2k\delta(k^2 - p^2 - q^2(p, n)). \tag{104}$$

Using the Poisson summation formula leads to the integration over the n variable, which can be performed explicitly. Letting $p = k\cos\theta$, one finds

$$\rho_b(k) = \frac{ak}{2\pi^2}\sum_{N=-\infty}^{+\infty}\int_0^{\pi} d\theta \left[b + \frac{1}{k}\tan(\frac{\phi_c(\theta)}{2})\right] e^{iN\phi_c(\theta)}e^{i2kbN\sin\theta}, \tag{105}$$

where ϕ_c is the phase shift due to clamping (15). In the semiclassical limit, the remaining integral can be evaluated using the stationary phase approximation, whose dominant contribution is found around $\theta = \pi/2$. Then, at the leading order, the oscillatory contribution to the staircase function is

$$N_b^{(osc)}(k) = \frac{1}{2\pi^{3/2}}a\sqrt{\frac{k}{b}}\sum_{N=1}^{\infty}\frac{1}{N^{3/2}}\cos(2Nbk - N\frac{\pi}{2} - \frac{3\pi}{4}). \tag{106}$$

Note that higher order terms also can be computed. Subtracting this from the previously obtained oscillating staircase function eliminates the large scale regular oscillation (see Fig. 10).

6.3 Oscillatory part of the density of states

As for the disk, we look to the Fourier transform of the density of states (with the weight $\sin(\pi k/k_{max})/k$ which gives sharper results) to check the semiclassical trace formula obtained in Section 4. If we compare it with the Dirichlet odd-odd membrane spectrum (596 levels for $k \leq 100$), only the semiclassical phase should be found different.

On Fig. 11, the comparison is made for $|F[\rho]|^2$. The periodic orbits indicated are those whose amplitude are the greatest in the trace formula : we have limited ourselves to the lowest values of the trace of the monodromy matrix. Each time the orbit is isolated in length, the agreement between the two curves is excellent. As length increases, close orbits make the different peaks interact, and due to their different phases, the shape of the composite peak differ between the two curves.

The main point is to verify that semiclassical phases are correct. The real part of $e^{-i\Phi_p}F[\rho]$ where Φ_p denotes the phase without the Maslov index contribution should be the same around the periodic orbit length l_p for the membrane and the plate. These comparisons are plotted on Fig. 12 for the first shortest orbits. The very good agreement shows the adequacy of the semiclassical derivation at this level.

6.4 Statistics of spectra

The membrane stadium spectrum is numerically known to have a statistical behavior at short scale well described by the random matrix Gaussian orthogonal ensemble (GOE) [22]. The nearest neighbor spacing distribution $P(s)$ in this case is close to the Wigner surmise

$$P_{GOE}(s) = \frac{\pi}{2} s e^{-\frac{\pi}{4}s^2} \tag{107}$$

On Fig. 13 is plotted $P(s)$ for the clamped plate, showing the same behavior here. This conclusion was first obtained in [9], from about the first 100 levels. An heuristic argument follows from the analogy at high energy between the membrane and the plate discussed in Section 2.

On Fig. 14 is represented the second moment of the statistics of the staircase fluctuations. For membranes, and the demonstration applies to plates, it has been shown [20] that

$$< \delta^2 > (k) = \frac{1}{\pi^2} \log(\frac{k}{\bar{\rho}(k^2)}) \tag{108}$$

as $k \to \infty$ for two-dimensional generic ergodic billiards. This is what is observed when the bouncing ball orbits contribution is suppressed. However, the behavior seems analytically the same with this contribution.

As a general conclusion, it can be said that Random Matrix Theory applies also to plates. Let us remark that about half a century ago (see [9] and references therein), it was argued that RMT should help describing spectral properties in various fields such as elasticity and acoustics.

7 Conclusion

In this paper, we have studied the fourth order biharmonic equation of flexural vibrations of elastic plates in the same semiclassical way as the membrane or quantum billiard problem is approached. In our case, exponential waves decreasing from the boundary are added to the classical propagating ones. The influence of this essential new feature is measured on the spectrum, more precisely on the mean number of levels and on its oscillatory part, and also on the statistical properties.

The surface and perimeter terms of the asymptotic number of levels are derived following the method of Balian and Bloch [14], independently from the rigorous derivation of Vasil'ev [15]. The next constant term, made of curvature and corner contributions, is also obtained.

A semiclassical approximation of the quantization condition is derived, containing, compared to the one for the membrane problem, an additional phase factor due to the phase shift of waves when reflected from the boundary of the plate. From this, a Berry-Tabor formula is obtained for the integrable disk case, and a Gutzwiller trace formula for chaotic ones. The first 600 eigenvalues for a clamped stadium plate have been obtained with an original numerical algorithm specially developed. The comparison of the Fourier transformed periodic orbits quantization formulas with the ones of a membrane with Dirichlet boundary conditions assess these derivations. For free plates, extra modes exponentially decaying from the boundary take place, giving extra peaks in the Fourier transform. The statistical properties of the spectrum appear to be the same as for the quantum billiard case.

The method we have used can easily be generalized for other models of wave propagation. The main ingredient is the construction of the exact scattering matrix from the straight boundary, which serves for two purposes. First, via the Krein formula, it defines the second term of the Weyl expansion of the mean level density and, second, it determines the leading order term of the trace formula.

Acknowledgments

The authors are greatly indebted to C. Schmit for numerous fruitful discussions and for providing the membrane stadium spectrum. We also thank S. Tomsovic for providing the periodic orbits of the stadium. One of the authors (E.H.) was supported by the French Ministry of Research.

Appendix A : Spectral shift function for one dimensional problems

The purpose of this appendix is the derivation of the simplest version of the general Krein formula (see [16]) which is very convenient in many cases and, in particular, for the derivation of the second term of the Weyl expansion discussed in Section 3 (on other applications of this formula for certain problems of quantum chaos see [24]).

Let H and H_0 be two self-adjoint spectral problems such that their difference $V = H - H_0$ is in some sense small. The typical situation is the case when H and H_0 are two Hamiltonians with different bounded potentials or two Hamiltonians with different boundary conditions. Then the Krein formula states that for an "arbitrary" test function ϕ

$$tr(\phi(H) - \phi(H_0)) = -\int \phi'(\mu)\xi(\mu)d\mu, \tag{109}$$

where the function ξ called the spectral shift function does not depends on the test function and is connected with the scattering matrix S

$$\det S(\lambda) = e^{i2\pi\xi(\lambda)}. \tag{110}$$

Ignoring problems with convergence Eq. (109) can be rewritten in the simple form

$$\Delta\rho(\lambda) \equiv \rho_H(\lambda) - \rho_{H_0}(\lambda) = \frac{d\xi(\lambda)}{d\lambda}, \tag{111}$$

where ρ_H is the density of states for the problem H

$$\rho_H(\lambda) = tr[\delta(\lambda - \hat{H})] = \sum_{n=1}^{+\infty} \delta(\lambda - \lambda_n^H),$$

and λ_n^H are eigenvalues of the spectral problem $\hat{H}\psi_n^H = \lambda_n^H \psi_n^H$ with the correct boundary conditions.

The importance of such formula comes from the fact that it permits to compute easily the change of the density of states under "small" changing of potential or boundary conditions (or both).

For clarity we sketch the formal derivation of this formula in the case of one-dimensional operators with constant coefficients of the type discussed in

Section 3 where all steps can be done without general theorems. The general derivation (but not the proving) follows a similar scheme (see [16], [15]).

Let $h(\hat{q})$ be a self-adjoint operator where $\hat{q} = -id/dy$. One can consider it e.g. as a real polynomial

$$h(\hat{q}) = \sum_{n=0}^{2m} a_n \hat{q}^n. \tag{112}$$

where $a_{2m} > 0$. The operator H_0 corresponds to the spectral problem

$$h(\hat{q})u = \lambda u \tag{113}$$

on the whole line $-\infty < y < \infty$ and the operator H will correspond to the same spectral problem but on the semi-interval $0 \le y < \infty$ with self-adjoint boundary conditions

$$(\hat{B}_j u)(0) = 0 \quad j = 1, \ldots, m, \tag{114}$$

with certain operators $\hat{B}_j$. Note that the number of different boundary conditions for an elliptic operator of degree $2m$ equals m.

In the case of plate vibration $h(q) = (q^2 + p^2)^2$ and the $\hat{B}_j$'s, for standard boundary conditions, are obtained from (9)-(11) taking only the leading order derivatives, and replacing $\partial/\partial l$ by ip and $\partial/\partial n$ by $i\hat{q}$.

The spectral problem admits the plane wave solutions of the type $e^{iq(\lambda)y}$ where $q(\lambda)$ satisfies the equation

$$h(q(\lambda)) = \lambda. \tag{115}$$

For a given value of λ, let us assume that this equation has $2d(\lambda)$ real solutions $q_r(\lambda)$, $r = 1, \ldots, 2d$. As the power of $h(q)$ is $2m$ and as $h(\hat{q})$ is assumed self-adjoint, the $2(m-d)$ complex roots can be divided in pairs with different sign of the imaginary part $q_c^{(\pm)}(\lambda) = a_c \pm i b_c$ with $b_c > 0$ and $c = 1, \ldots, m-d$.

Assuming that all real roots are different one can divide them into two intertwining classes $q_r^{(-)}$ and $q_r^{(+)}$ with $r = 1, \ldots, d$, such that

$$q_1^{(-)} < q_1^{(+)} < q_2^{(-)} < q_2^{(+)} < \ldots < q_d^{(+)}.$$

$q_r^{(+)}$ is a root for which $h'(q) > 0$ and $q_r^{(-)}$ for which $h'(q) < 0$. The number d is called the multiplicity of the eigenvalue λ.

Let us define the current operator $\hat{J}$ by the condition

$$g[h(\hat{q})f] - [\overline{h(\hat{q})g}]f = \hat{q}[g\hat{J}f]. \qquad (116)$$

The explicit form of $\hat{J}$ follows from the identity

$$g\hat{q}^n f - f\overline{\hat{q}}^n g = \hat{q}\sum_{k=0}^{n-1} \overline{\hat{q}}^k g\hat{q}^{n-1-k} f.$$

It is easy to check that for every plane wave solution e^{iqy} the value of the current is

$$e^{-iqy}\hat{J}e^{iqy} = h'(q). \qquad (117)$$

The above mentioned two types of real roots correspond to two different types of waves: $q_r^{(-)}$ can be interpreted as wavevectors for incoming waves and $q_r^{(+)}$ correspond to outcoming waves.

The Green function of the free problem H_0 can be expressed by the usual formula

$$G_0^{\pm}(y, y'; \lambda) = \frac{1}{2\pi}\int_{-\infty}^{+\infty} \frac{e^{iq(y-y')}}{h(q) - \lambda \mp i\varepsilon} dq, \qquad (118)$$

and its discontinuity $\Delta G_0(y, y'; \lambda) \equiv G_0^+(y, y'; \lambda) - G_0^-(y, y'; \lambda)$ equals

$$\Delta G_0(y, y'; \lambda) = i\sum_{r=1}^{d}\left[\frac{e^{iq_r^{(+)}(y-y')}}{|h'(q_r^{(+)})|} + \frac{e^{iq_r^{(-)}(y-y')}}{|h'(q_r^{(-)})|}\right], \qquad (119)$$

where $q_r^{(\pm)}$ are real solutions of (115).

Let $u_j(y; \lambda)$ be the j^{th} eigenfunction of the spectral problem (113) with boundary conditions (114). If all solutions of (115) are different, each eigenfunction have the form

$$u_j(x; \lambda) = \frac{1}{\sqrt{2\pi}}\sum_{r=1}^{d}\left[C_{jr}^{(-)}\frac{e^{iq_r^{(-)}y}}{|h'(q_r^{(-)})|^{1/2}} + C_{jr}^{(+)}\frac{e^{iq_r^{(+)}y}}{|h'(q_r^{(+)})|^{1/2}}\right] + \sum_{c=1}^{m-d} B_{jc}e^{-b_c y}e^{ia_c y}, \qquad (120)$$

where the first sum is the expansion over the incoming and outcoming waves, and the second one is the expansion over the complex admissible wavevectors $q_c^{(+)}$, the latter giving solutions decaying as $y \to +\infty$.

All coefficients $C_{jr}^{(\pm)}$ and B_{jc} have to be determined from the boundary conditions (114). As the number of boundary operators is m and the number of unknowns is $2d+(m-d)=m+d$ in general one gets d linear independent solutions $u_j(y;\lambda)$, $j=1,\ldots,d$. From physical considerations it is clear (and can be easily checked from the current conservation) that the amplitudes of incoming waves $C_{jr}^{(-)}$ can be chosen as an arbitrary (unitary) matrix and the amplitudes of outcoming waves $C_{jr}^{(+)}$ will be connected to them by a unitary matrix S

$$C^{(+)}=SC^{(-)}, \tag{121}$$

which is obviously called the scattering matrix. Direct verification shows that for a unitary matrix $C^{(-)}$ the factors in (120) ensure that the functions $u_j(y;\lambda)$ are normalized in the following way

$$\int \bar{u}_j(y;\lambda)u_{j'}(y';\lambda)d\lambda=\delta_{jj'}\delta(y-y'). \tag{122}$$

The knowledge of eigenfunctions of the spectral problem permits to compute the Green function by the usual formula

$$G^{\pm}(y,y';\lambda)=\sum_n \frac{\bar{u}_n(y')u_n(y)}{\lambda_n-\lambda\pm i\varepsilon}, \tag{123}$$

where the sum is taken on both the continuous and discrete spectra. In particular

$$\Delta G(y,y';\lambda)=2\pi i\sum_{j=1}^{d}\bar{u}_j(y';\lambda)u_j(y;\lambda)+2\pi i\sum_k \delta(\lambda_k-\lambda)\bar{u}_k(y')u_k(y), \tag{124}$$

where the second sum extends on the purely discrete spectrum for which $C^{(\pm)}=0$. These eigenfunctions are normalized to 1.

The change of the density of states defined in (111) equals

$$\Delta\rho(\lambda)=\frac{1}{2\pi i}\int_0^{+\infty}(\Delta G(y,y;\lambda)-\Delta G_0(y,y;\lambda))dy. \tag{125}$$

Substituting expressions (119) and (124) into this formula, where a factor $\exp(-\alpha y)$ is introduced for convergence, one obtains

$$\begin{aligned}\Delta\rho(\lambda) &= \lim_{\alpha\to 0+}[\sum_{j=1}^{d}\int_0^{+\infty}|u_j(y;\lambda)|^2 e^{-\alpha y}dy \\ &- \frac{1}{2\pi\alpha}\sum_{j=1}^{d}(\frac{1}{|h'(q_r^{(+)})|}+\frac{1}{|h'(q_r^{(-)})|})]+\sum_k\delta(\lambda_k-\lambda).\end{aligned} \tag{126}$$

To compute the integral

$$\sum_j \int_0^{+\infty} |u_j(y;\lambda)|^2 e^{-\alpha y} dy$$

it is convenient to use the following trick (see e.g. [15]). By differentiating the equation

$$h(\hat{q}) u_j(y;\lambda) = \lambda u_j(y;\lambda)$$

with respect to λ, one gets

$$u_j(y;\lambda) = [h(\hat{q}) - \lambda] \frac{\partial u_j(y;\lambda)}{\partial \lambda}.$$

From (116) it follows that

$$\bar{u}_j u_j = \bar{u}_j [h(\hat{q}) - \lambda] \frac{\partial u_j}{\partial \lambda} = \overline{[h(\hat{q}) - \lambda] u_j} u \frac{\partial u_j}{\partial \lambda} - i \frac{d}{dx} (\bar{u}_j \hat{J} \frac{\partial u_j}{\partial \lambda}),$$

and

$$\int_0^{+\infty} |u_j|^2 e^{-\alpha y} dy = -i\alpha \int_0^{+\infty} \bar{u}_j \hat{J} \frac{\partial u_j}{\partial \lambda} e^{-\alpha y} dy.$$

As $\alpha \to 0^+$ only terms of negative power of α can contribute. But they can come only from the integrand proportional to 1 and y. In other words, only terms coming from the interference of plane waves with exactly the same values of $q(\lambda)$ are important. Taking into account of (117) and that

$$h'(q(\lambda)) \frac{dq}{d\lambda}(\lambda) = 1, \quad \text{and} \quad e^{-iqy} (\hat{J} y - y \hat{J}) e^{iqy} = -i \frac{h''(q)}{2},$$

one obtains

$$\begin{aligned} 2\pi \sum_{j=1}^{d} (\bar{u}_j \hat{J} \frac{\partial u_j}{\partial \lambda}) &= iy \sum_{j,r=1}^{d} \left[|C_{jr}^{(-)}|^2 \frac{1}{|h'(q_r^{(-)})|} + |C_{jr}^{(+)}|^2 \frac{1}{|h'(q_r^{(+)})|} \right] \\ &+ \sum_{j,r=1}^{d} \left[\overline{C}_{jr}^{(+)} \frac{dC_{jr}^{(+)}}{d\lambda} - \overline{C}_{jr}^{(-)} \frac{dC_{jr}^{(-)}}{d\lambda} \right]. \end{aligned}$$

As the matrices $C^{(\pm)}$ are unitary, the first term equals

$$\sum_{r=1}^{d} \left[\frac{1}{|h'(q_r^{(+)})|} + \frac{1}{|h'(q_r^{(-)})|} \right]$$

and after the integration it cancels with the same term from ΔG_0 (119) and the final formula reads

$$\begin{aligned}\Delta\rho(\lambda) &= \frac{1}{2\pi}tr(C^{(+)\dagger}\frac{dC^{(+)}}{d\lambda} - C^{(-)\dagger}\frac{dC^{(-)}}{d\lambda}) + \sum_k \delta(\lambda_k - \lambda)\\ &= \frac{1}{2\pi}tr(S^\dagger\frac{dS}{d\lambda}) + \sum_k \delta(\lambda_k - \lambda),\end{aligned} \tag{127}$$

where the scattering matrix S is defined in (121). Introducing the spectral shift function ξ by the relation

$$\xi(\lambda) = \frac{1}{2\pi}\text{Arg det } S(\lambda), \tag{128}$$

one immediately concludes that

$$\Delta\rho(\lambda) = \frac{d\xi}{d\lambda}(\lambda) + \sum_k \delta(\lambda_k - \lambda), \tag{129}$$

and the change of the staircase functions is

$$\Delta N(\lambda) = \xi(\lambda) + n_{d.s.}(\lambda). \tag{130}$$

The second term in these formulae is connected with discrete spectrum of H. (If H_0 also has a discrete spectrum the modification of this formula is obvious.)

In the derivation of this formula it was assumed that all q_j are different. The points λ_* where the equation $h(q) = \lambda_*$ has a multiple real root are called singular points of the continuous spectrum. In these points the dimension of the scattering matrix changes and they give δ-function singularities in $\Delta\rho$ or a jump in function ξ. In the most common case of the appearance of an eigenvalue of multiplicity 2

$$\xi(\lambda_* + 0) - \xi(\lambda_* - 0) = -\frac{1}{4}. \tag{131}$$

The general case is discussed in details in [15].

Using (130) the second term of the Weyl expansion of the smooth staircase function for two-dimensional problems can be written in the form

$$\bar{N}_2(\lambda) = L\int_{-\infty}^{+\infty}\frac{dp}{2\pi}(\xi(\lambda,p) + n(\lambda,p)), \tag{132}$$

where $\xi(\lambda, p)$ and $n(\lambda, p)$ are the spectral shift function and the number of states of the discrete spectrum for the one-dimensional straight-line boundary problem, and p is the momentum parallel to this boundary.

Appendix B : Curvature contribution

The general method for the computation of the higher order terms of the Weyl expansion for billiard problems with smooth boundaries has been developed in [17]. With obvious modifications it can be adapted as well for problems of plate vibration. We found that it is more convenient to use a slightly different method. As in [17], the Weyl expansion can be read off from the knowledge of the asymptotics, when $s \to \infty$, of the Green function corresponding to the (diffusion-type) equation

$$(\Delta_{\vec{r}}^2 + s^2)G(\vec{r}, \vec{r}\,'; s) = \delta(\vec{r} - \vec{r}\,'), \tag{133}$$

inside the domain $\mathcal{D}$, G obeying to the desired boundary condition on the contour $\mathcal{C}$.

Let the smooth part of the staircase function, $\tilde{N}(k)$, have the following Weyl expansion as $k \to \infty$

$$\tilde{N}(k) = \sum_{n=-N}^{2} c_n k^n. \tag{134}$$

If we consider

$$K(s) = \sum_n \frac{1}{k_n^4 + s^2} = \int_{\mathcal{D}} G(\vec{r}, \vec{r}; s) d\vec{r}, \tag{135}$$

then its asymptotical form as $s \to \infty$ is connected to the Weyl coefficients c_n by

$$K(s) \sim \sum_{n=-N}^{2} \frac{c_n}{s^{2-n/2}} \frac{\pi n}{4 \sin(\pi n/4)}. \tag{136}$$

In particular the beginning of this expansion is

$$K(s) \sim \frac{\pi}{2s} c_2 + \frac{\pi\sqrt{2}}{4s^{3/2}} c_1 + \frac{1}{s^2} c_0. \tag{137}$$

The free Green function of Eq. (133) is

$$G_0(\vec{r},\vec{r}\,';s) = \int \frac{dpdq}{(2\pi)^2} \frac{e^{ip(x-x')+iq(y-y')}}{(p^2+q^2)^2+s^2}. \tag{138}$$

Integrating over q, one gets the following expression

$$G_0(\vec{r},\vec{r}\,';s) = \frac{i}{8\pi s} \int e^{ip(x-x')} \left(\frac{1}{r_+} e^{-r_+|y-y'|} - \frac{1}{r_-} e^{-r_-|y-y'|} \right) dp, \tag{139}$$

where $r_\pm = \sqrt{p^2 \pm is}$.

The half-plane ($y \geq 0$) Green function which obeys the desired boundary conditions can be written (as in Section 3) as

$$G_{h.p.}(\vec{r},\vec{r}\,';s) = \frac{i}{8\pi s} \int e^{ip(x-x')} (\frac{1}{r_+} e^{-r_+|y-y'|} - \frac{1}{r_-} e^{-r_-|y-y'|} + A_+ e^{-r_+(y+y')}$$
$$+A_- e^{-r_-(y+y')} + B_+ e^{-r_+ y - r_- y'} + B_- e^{-r_- y - r_+ y'})dp. \tag{140}$$

where the coefficients $A_\pm$ and $B_\pm$ have to be determined from the boundary conditions. At this stage, we will focus on the clamped edge. Similar, but more tedious computations, can be done for a free edge. In the former case

$$G|_{y=0} = 0, \quad \frac{\partial G}{\partial y}|_{y=0} = 0, \tag{141}$$

and one obtains

$$A_\pm = \frac{r_+ + r_-}{r_+ - r_-} \frac{1}{r_\pm}, \quad B_\pm = -\frac{2}{r_+ - r_-}. \tag{142}$$

To find the contribution fron the curvature one has to construct the Green function which obeys the boundary condition not on the line $y = 0$ but on the 'circle' $y = x^2/2R$ where R is the local radius of curvature. We shall look for this function in the form similar to Eq. (140). Namely, we assume that it can be written in the following form

$$G(\vec{r},\vec{r}\,';s) = G_{h.p.}(\vec{r},\vec{r}\,';s) + \int e^{ip(x-x')} (D_+(p,y') e^{-r_+ y} + D_-(p,y') e^{-r_- y}) dp. \tag{143}$$

The function defined by this expresion obeys (133) for arbitrary functions $D_\pm(p, y')$, which have to be found from boundary conditions. As $G_{h.p.}(\vec{r},\vec{r}\,';s)$

obeys the boundary conditions at $y=0$, the functions $D_{\pm}(p,y')$ can be determined by perturbation theory for large s. We shall perform the calculation for the clamped boundary conditions

$$G|_{y=x^2/2R}=0,\ \frac{\partial G}{\partial n}|_{y=x^2/2R}=0. \tag{144}$$

Putting $x'=0$ and taking into account that the normal derivative at the point x is

$$\frac{\partial}{\partial n}=\cos\theta\frac{\partial}{\partial y}-\sin\theta\frac{\partial}{\partial x},$$

where $\sin\theta=x/R$ one gets that in the leading order functions $D_{\pm}(p,y')$ fulfil the following equations

$$\int e^{ipx}(D_{+}(p,y')+D_{-}(p,y'))dp=0, \tag{145}$$

and

$$\int e^{ipx}(D_{+}(p,y')r_{+}+D_{-}(p,y')r_{-})dp=\frac{x^2}{2R}\frac{\partial^2 G_{h.p}}{\partial y^2}|_{y=0}. \tag{146}$$

Their solution is

$$D_{+}(p,y')=-D_{-}(p,y')=\mu(p,y'), \tag{147}$$

and

$$\mu(p,y')=-\frac{i}{8\pi sR}\frac{1}{r_{+}-r_{-}}\frac{\partial^2}{\partial p^2}\left[(r_{+}+r_{-})(e^{-r_{+}y'}-e^{-r_{-}y'}\right]. \tag{148}$$

The function $K(s)$ in (135) can be expressed as follows (see [17])

$$K(s)=\int_C dl\int_0^{+\infty}dyG(x,y;x,y;s)(1-\frac{y}{R(l)}), \tag{149}$$

where l denotes the coordinate along the boundary C.

At the leading order in R (or s), the third term of the Weyl expansion can be written as the sum of two integrals

$$K_3(s)=(I_1+I_2)\int_C\frac{dl}{R(l)}, \tag{150}$$

where

$$I_1 = -\frac{i}{8\pi s}\int dp\int_0^{+\infty} ydy\left[\frac{r_+ + r_-}{r_+ - r_-}(\frac{e^{-2r_+y}}{r_+} + \frac{e^{-2r_-y}}{r_-}) - \frac{4}{r_+ - r_-}e^{-(r_+ + r_-)y}\right], \tag{151}$$

and

$$I_2 = -\frac{i}{8\pi s}\int dp\int_0^{+\infty} dy\left[\frac{e^{-r_+y} - e^{-r_+y}}{r_+ - r_-}\frac{\partial^2}{\partial p^2}\left((r_+ + r_-)(e^{-r_+y} - e^{-r_-y}\right)\right]. \tag{152}$$

After some algebra we obtain

$$I_1 + I_2 = \frac{1}{4\pi}\int dp(\frac{r_+^5 + r_-^5}{8(r_+r_-)^5} - \frac{2}{r_+r_-(r_+ + r_-)^3}). \tag{153}$$

Introducing the angle ϕ from the condition $\tan\phi = s/p^2$ this integral can be transformed as follows

$$\begin{aligned} I_1 + I_2 &= \frac{1}{16\pi s^2}\int_0^{\pi/2} d\phi\frac{\sin\phi}{\sqrt{\cos\phi}\cos^3\phi/2}(1 - \cos^3\phi/2\cos 5\phi/2) \\ &= -\frac{1}{48\pi s^2}\frac{\sqrt{\cos\phi}}{\cos\phi/2}(15 - 2\cos^3\theta - \cos^2\theta + 4\cos\theta)|_{\theta=0}^{\theta=\pi/2} \\ &= \frac{1}{3\pi s^2}. \end{aligned} \tag{154}$$

Comparing it with (137), one concludes that the third term of the Weyl expansion connected with the curvature of the boundary is

$$c_0^c = \frac{1}{3\pi}\int_C \frac{dl}{R(l)}. \tag{155}$$

Note that for the membrane the corresponding coefficient equals $1/12\pi$.

Appendix C : Numerical solution of the biharmonic equation

We found that it is convenient to represent solutions of the biharmonic equation in the following form

$$W(\vec{r}) = \sum_{m=-\infty}^{+\infty} c_m J_m(kr)e^{im\theta} + \int_C K_0(k|\vec{r} - \vec{r}(s)|)\mu(s)ds, \tag{156}$$

where C is the frontier of the plate, and K_0 is the modified Bessel function. The first term is the general solution of the Helmholtz equation in the polar coordinates (r,θ), written in the form of a series, which has been proven to be an efficient numerical formulation for the membrane problem. The second is a solution of the equation $(\Delta - k^2)W = 0$, written as a boundary integral or single layer potential, with distribution function μ. As $K_0(x) \sim \sqrt{\pi/2x}\exp(-x)$ when $x \to +\infty$, the integral is thought to behave well at high energies. The choice of writing this part as the first part of the solution, as a series of hyperbolic Bessel functions $I_m(kr)$ has previously been tried in [9], but leads rapidly to numerical divergence problems due to the exponentially increasing behavior of these functions for large argument.

The solution of the problem, that is the determination of the unknown coefficients c_m and of the function μ, is obtained writing that (156) satisfies the boundary conditions. We have considered here only the case of clamping, which leads to the following system, for any point $\vec{r}(t)$ on the frontier

$$\sum_{m=-\infty}^{+\infty} c_m J_m(kr(t))e^{im\theta(t)} + \int_C K_0(k|\vec{r}(t)-\vec{r}(s)|)\mu(s)ds = 0, \qquad (157)$$

$$\sum_{m=-\infty}^{+\infty} c_m \left[kJ'_m(kr(t))\cos\alpha(t) + i\frac{m}{r(t)}J_m(kr(t))\sin\alpha(t)\right]e^{im\theta(t)} +$$
$$\pi\mu(t) - \int_C K_1(k|\vec{r}(t)-\vec{r}(s)|)k\frac{[\vec{r}(t)-\vec{r}(s)]\cdot\vec{n}(t)}{|\vec{r}(t)-\vec{r}(s)|}\mu(s)ds = 0. \qquad (158)$$

$\vec{n}(t)$ is the outward normal at point t, which makes an angle $\alpha(t)$ with $\vec{r}(t)$. It is well known (see e.g. [27]) that the single layer potential is continuous across the frontier C, and that the double layer potential is discontinuous (see 64)), leading to the extra term $\pi\mu(t)$ in (158).

Numerically, we can only impose these previous conditions at a finite number of points and for a finite number of unknowns. From the well-known property that $J_m(x) \to 0$ as $m \to +\infty$, the series can be truncated to $|m| \leq M = E[kr_{max}]+M_0$ ($M_0 = 0,1,2,3$) where r_{max} is the maximum value of r. The boundary integral is discretized using N points regularly spaced on the frontier C, giving the unknowns μ_n, $n = 1,\ldots,N$. We impose the equalities (157) and (158) to be satisfied at P points regularly spaced on the frontier. To be soluble, the parameters of this finite system must satisfy the condition $2P = M + N$ for the particular case of odd solutions with respect to θ, which will be the case below. To control the error term of the algorithm, it is convenient to choose the P evaluation points at regular distance from the N discretization points : in other words, we impose $N = (2p-1)M$, where p is an integer, and then $P = pM$. The function K_0 has a logarithmic singularity at small distances, and to be handled with precision, one should take enough points around it. Numerically, $p = 3$ has been proven to give a sufficient accuracy for the eigenvalues, if the boundary integral containing K_0 is furthermore integrated by parts -integrating μ- to diminish the effects of the singularity.

We obtain a linear system of $2P$ equations with $2P$ unknowns, which possesses a non trivial solution when k is an eigenvalue, that is when the determinant of the system vanishes. The method determines the optimal number of unknowns for a range in k, and calculates the determinant as a function of k.

In the computation for the quarter of a stadium, symmetry has been taken into account to reduce the number of points. The determinant has been written such as to be real, and has been found to oscillate, having zeroes in between. Several precision tests have determined the accuracy of the computed eigenvalues to be of the order of $\Delta k^2/50$, where Δk is the mean level spacing.

References

[1] M. C. Gutzwiller, J. Math.Phys. **12**, 343 (1971).

[2] Chaos and quantum physics, Proc. of Les Houches Summer School of Theoretical Physics, 1989 (Eds. M.-J. Giannoni, A. Voros, and Zinn-Justin), (North Holland, Amsterdam, 1991).

[3] L. D. Landau and E. M. Lifshitz, *Theory of elasticity*, (Pergamon Press, London, 1959).

[4] A. E. H. Love, *A treatise on the mathematical theory of elasticity*, (Dover, New York, 1944).

[5] J. D. Achenbach, *Wave propagation in elastic solids*, Series in Applied Mathematics and Mechanics, Vol. 16, (North Holland, 2nd ed., Amsterdam, 1976).

[6] K. F. Graff, *Wave motion in elastic solids*, (Dover, New York, 1991).

[7] R. L. Weaver, J. Acoust. Soc. Am. **85**, (3) 1005 (1989); O. Bohigas, O. Legrand, C. Schmit and D. Sornette, J. Acoust. Soc. Am. **89**, (3) 1456 (1991); D. Delande, D. Sornette and R. Weaver, J. Acoust. Soc. Am. **96**, (3) 1873 (1994).

[8] C. Ellegaard, T. Guhr, K. Lindemann, H. Q. Lorensen, J. Nygård and M. Oxborrow, Phys. Rev. Lett. **75**, 1546 (1995); M. Oxborrow and C. Ellegaard, *Proceedings of the 3rd International Conference on Experimental Chaos* (World Scientific, Edinburgh), to be published; C. Ellegaard, T. Guhr, K. Lindemann, J. Nygård and M. Oxborrow, Proceedings of the IV^{th} Wigner Symposium in Guadalajara, Mexico, ed. N. M. Alakishiyev, T. H. Seligman and K. B. Wolf, World Scientific, Singapore (1996) pp 330-333; C. Ellegaard, T. Guhr, K. Lindemann, J. Nygård and M. Oxborrow, Phys. Rev. Lett., to appear.

[9] O. Legrand, C. Schmit and D. Sornette,*Europhys. Lett.* **18**, 101 (1992).

[10] L. Couchman, E. Ott and T. M. Antonsen, Jr, Phys. Rev. A **46**, 6193 (1992); L. S. Schuetz, PhD Thesis, University of Maryland (1991).

[11] R. E. Prange, E. Ott, T. M. Antonsen, Jr., B. Georgeot and R. Blümel, Phys. Rev. E **53**, 207 (1996); R. Blümel, T. M. Antonsen, Jr, B. Georgeot, E. Ott and R. E. Prange, Phys. Rev. Lett. **76**, 2476 (1996).

[12] P. Bertelsen, C. Ellegaard and E. Hugues, to be published.

[13] G. Chen, M. P. Coleman and J, Zhou, SIAM J. Appl. Math. **51**, (4) 967 (1991).

[14] R. Balian and C. Bloch, Ann. Phys. **60**. 401 (1970).

[15] D. G. Vasil'ev, Trans. Moscow Math. Soc. **49**, 173 (1987).

[16] M. Sh. Birman and D.R. Yafaev, St. Petersburg Math. J. **4**, 833 (1993).

[17] K. Stewartson and R.T. Waechter, Proc. Cambridge Phil. Soc. **69**, 353 (1971).

[18] M. V. Berry and M. Tabor, Proc. R. Soc. Lond. A **349**, 101 (1976).

[19] M. V. Berry and M. Tabor, J. Phys. A: Math. Gen. **10**, 371 (1977).

[20] E. Bogomolny and C. Schmit, Nonlinearity **6**, 523 (1993).

[21] L. A. Bunimovich, Commun. Math. Phys. **65** 295 (1979); L. A. Bunimovich, Chaos **1** 187 (1991).

[22] O. Bohigas, M. J. Giannoni and C. Schmit, Phys. Rev. Lett. **52**, 1 (1984).

[23] M. Sieber, H. Primack, U. Smilansky, I. Ussishkin and H. Schanz, J. Phys. A: Math. Gen. **28**, 5041 (1995).

[24] U. Smilansky and I. Ussishkin, J. Phys. A: Math. Gen. **29**, 2587 (1996).

[25] E. B. Bogomolny, Nonlinearity **5**, 805 (1992).

[26] B. Georgeot and R. E. Prange, Phys. Rev. Lett. **74**, 2851 (1995); B. Georgeot and R. E. Prange, *ibid.* **74**, 4110 (1995).

[27] V.I. Smirnov, *A course of Higher Mathematics* Vol. IV, (Pergamon Press, 1964).

FIGURE CAPTIONS

Figure 1 : Reflection of waves for a straight boundary in the case $k < |p|$.
Figure 2 : Variation of the phase shift ϕ with respect to the incidence angle θ for the clamped plate (continuous line) and the free plate (dashed lines) for $\nu = 0.1$ (lower), $\nu = 0.3$ (middle) and $\nu = 0.5$ (upper).
Figure 3 : Difference between the staircase function and its mean part for the clamped disk plate spectrum as a function of k.
Figure 4 : Same as Fig. 3 for the free disk plate for $\nu = 0.5$.
Figure 5 : Real part of $e^{-i\Phi_p}F[\rho]$ as a function of l for the clamped disk plate spectrum. The semiclassical phase has been eliminated for each periodic orbit to get pure Gaussian peaks. The crosses indicate the semiclassical amplitudes.
Figure 6 : $|F[\rho]|^2$ as a function of l for the free disk plate spectra ($\nu = 0.5$), for all modes (dotted line), boundary modes (dashed line) and all modes except boundary ones (continuous line). Crosses indicate semiclassical amplitudes.
Figure 7 : $|F[\rho]|^2$ as a function of l for the disk spectra. The lower curve is for the Dirichlet membrane, the uppers for the clamped plate (dashed line) and free plate for $\nu = 0.5$ (continuous line). Crosses indicate the semiclassical amplitudes. *(a)* is for the winding number 1 orbits and *(b)* for the winding number 2 orbits.
Figure 8 : Nearest neighbor spacing distribution $P(s)$ for the Dirichlet membrane half-disk spectra (lower histogram), the clamped plate (shifted middle histogram) and the free plate for $\nu = 0.5$ (shifted upper histogram). The Poissonian distribution (dotted line) is shown for comparison.
Figure 9 : $< \delta^2 >$ as a function of N for the Dirichlet membrane disk spectra (lower curve), the clamped plate (shifted middle curve) and the free plate for $\nu = 0.5$ (shifted upper curve). The dashed line is the best fit in the form $C\sqrt{n}$ with $C_m^D = 0.1235$, $C_p^c = 0.1238$ and $C_p^f = 0.1262$.
Figure 10 : Difference between the staircase function and its mean part for the clamped stadium plate odd-odd spectrum as a function of k (upper continuous line), contribution of the neutral family of bouncing ball orbits (dashed line) and the difference of the two (shifted lower line).
Figure 11 : $|F[\rho]|^2$ as a function of l for the stadium odd-odd spectra: Dirichlet membrane (dashed line) and clamped plate (continuous line). Ver-

tical lines indicate the predominant periodic orbits in the trace formula. *(a)* is for the first peaks and *(b)* for the next ones.

Figure 12 : Real part of $e^{-i\Phi_p}F[\rho]$ as a function of l for different orbits for the stadium odd-odd spectra : Dirichlet membrane (dashed line) and clamped plate (continuous line). *(a)* $l = 1.3265$: bouncing ball ($\Phi^m = 315^o$, $\Phi^p = 225^o$). *(b)* $l = 2.9661$: diagonal ($\Phi^m = 0^o$, $\Phi^p = 244^o.67$). *(c)* $l = 3.4463$: bow tie ($\Phi^m = 180^o$, $\Phi^p = 28^o.96$); $l = 3.7519$: double diamond ($\Phi^m = 0^o$, $\Phi^p = 180^o$); $l = 3.9795$: bouncing ball repeated 3 times ($\Phi^m = 315^o$, $\Phi^p = 45^o$).

Figure 13 : Nearest neighbor spacing distribution $P(s)$ for the clamped stadium plate odd-odd spectrum. The Poissonian distribution (dotted line) and the $P_{GOE}(s)$ (dashed line) are shown for comparison.

Figure 14 : $< \delta^2 >$ as a function of N for the clamped odd-odd plate spectrum with (upper continuous line) the bouncing ball contribution, and its best fit (dotted line) for $N > 100$ in the form $a + b \log N$: $a = 0.1598$ and $b = 0.0410$. Without the bouncing ball contribution (lower curves) : $a = -0.0559$ and $b = 0.1075$.

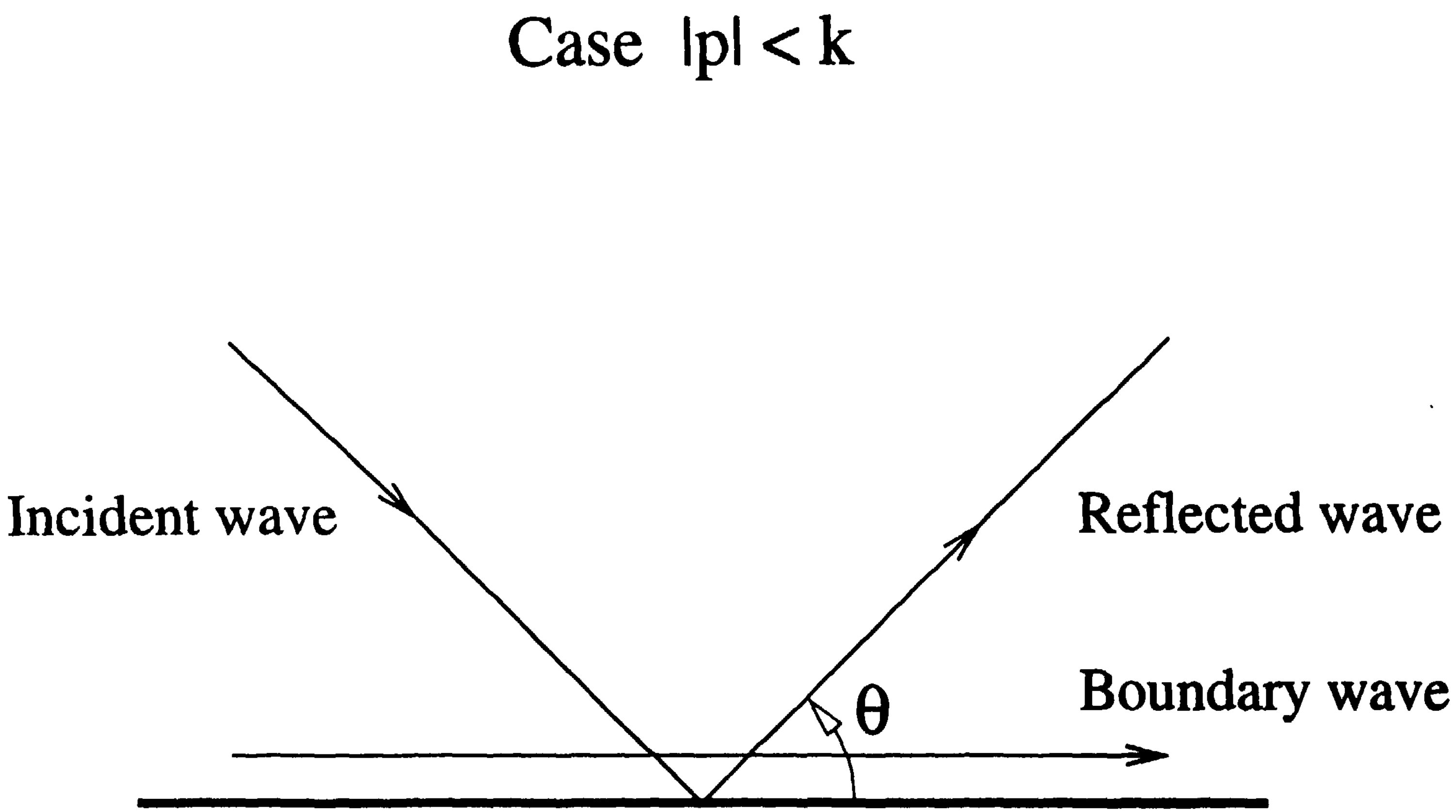

Fig. 1

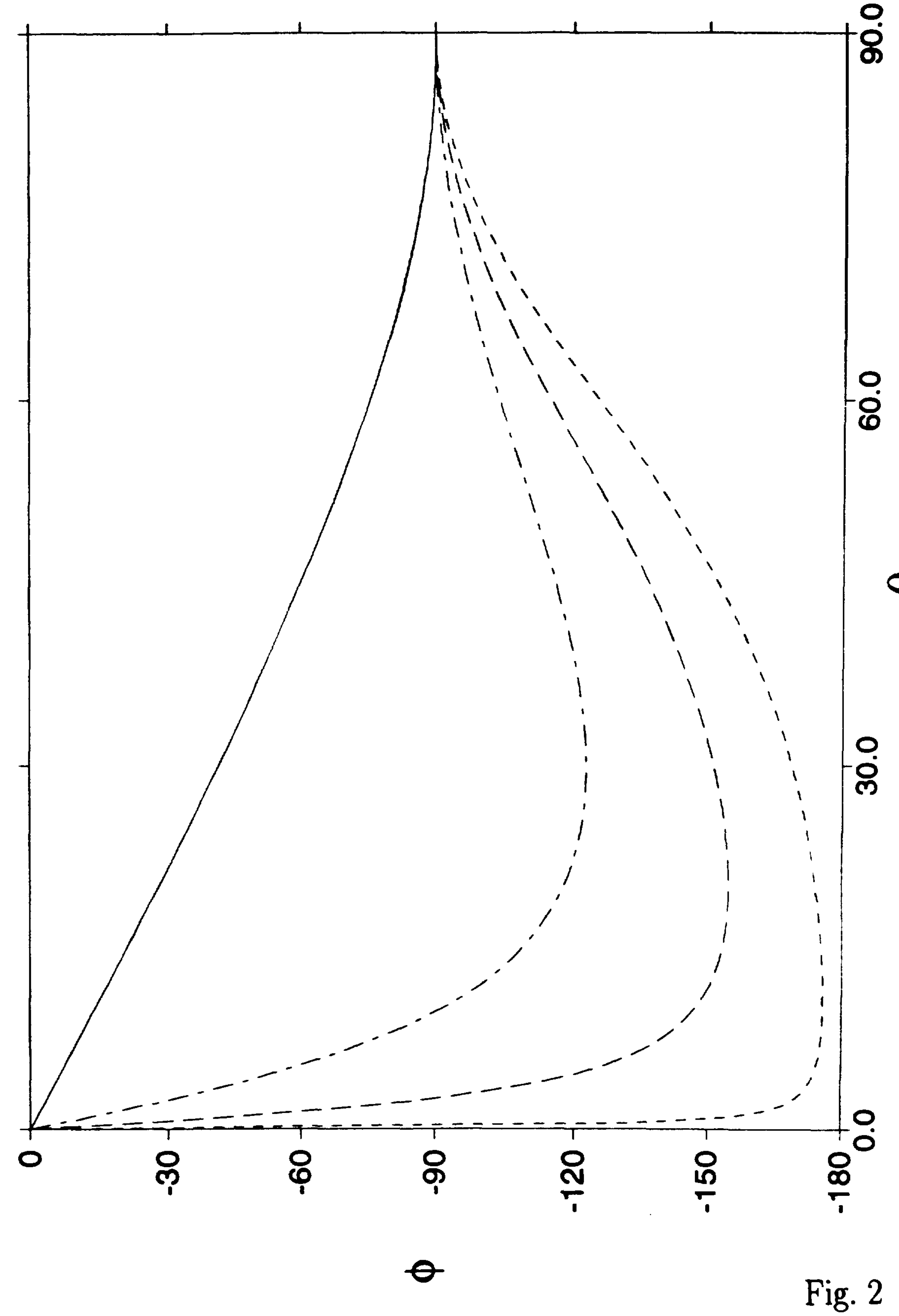

Fig. 2

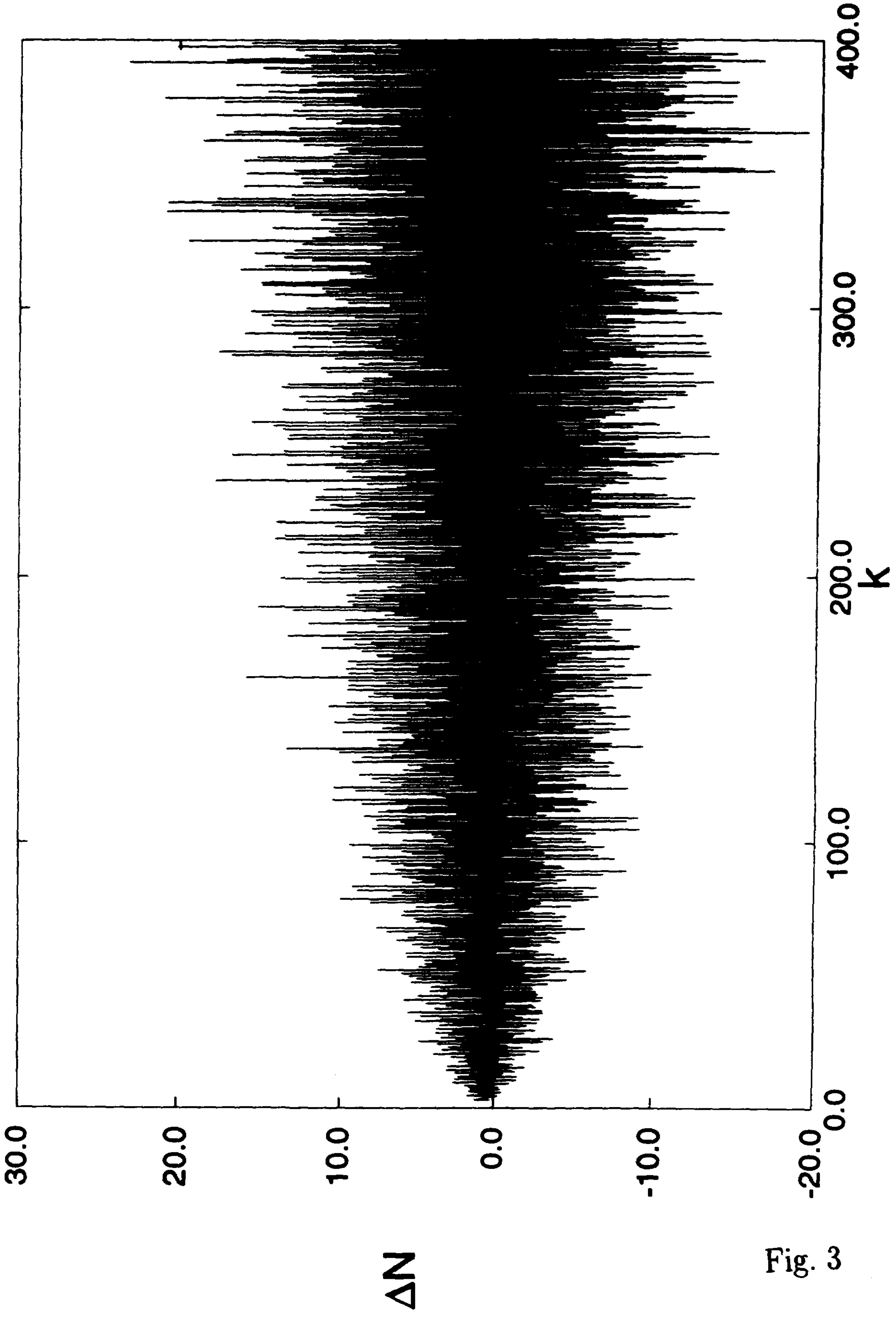

Fig. 3

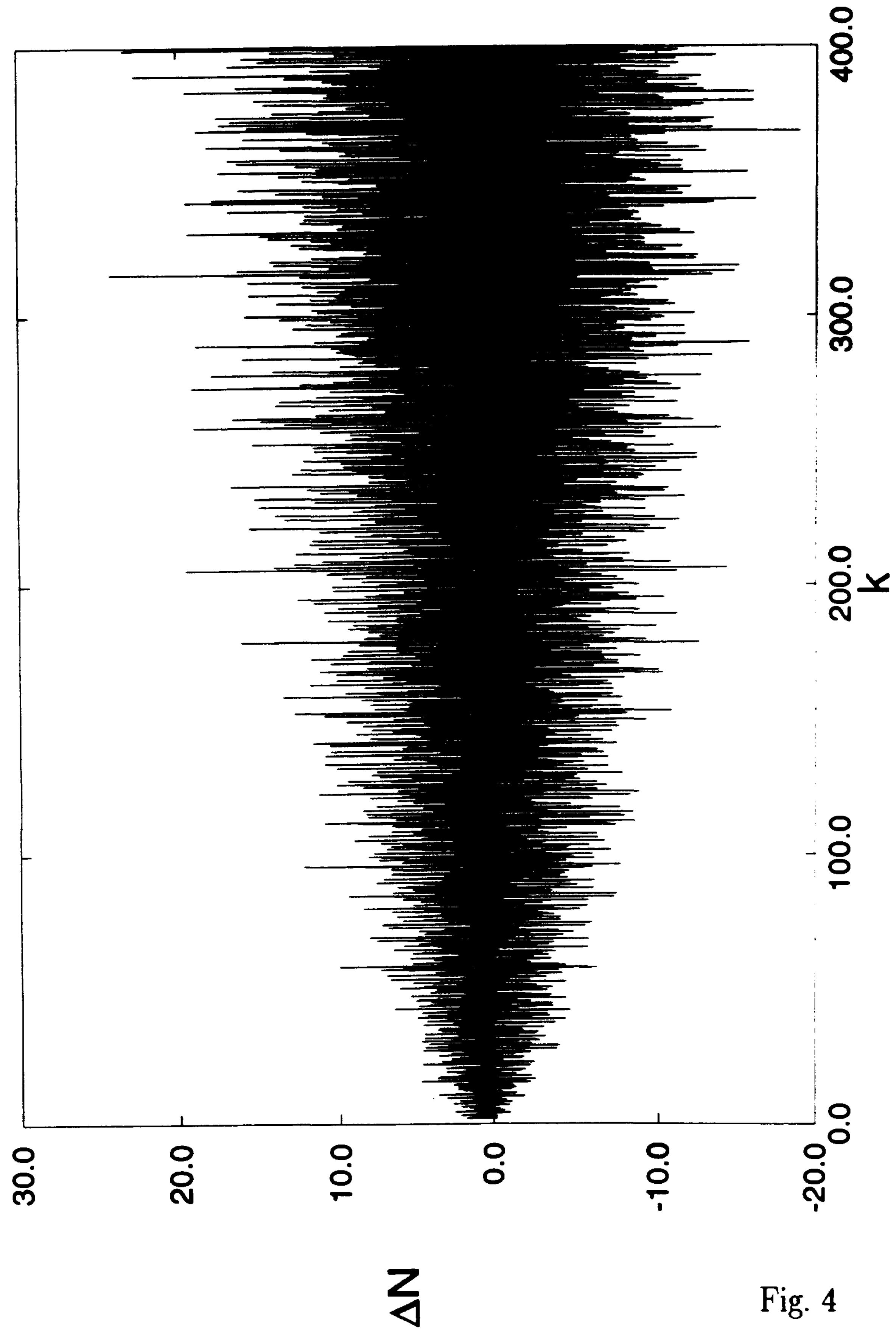

Fig. 4

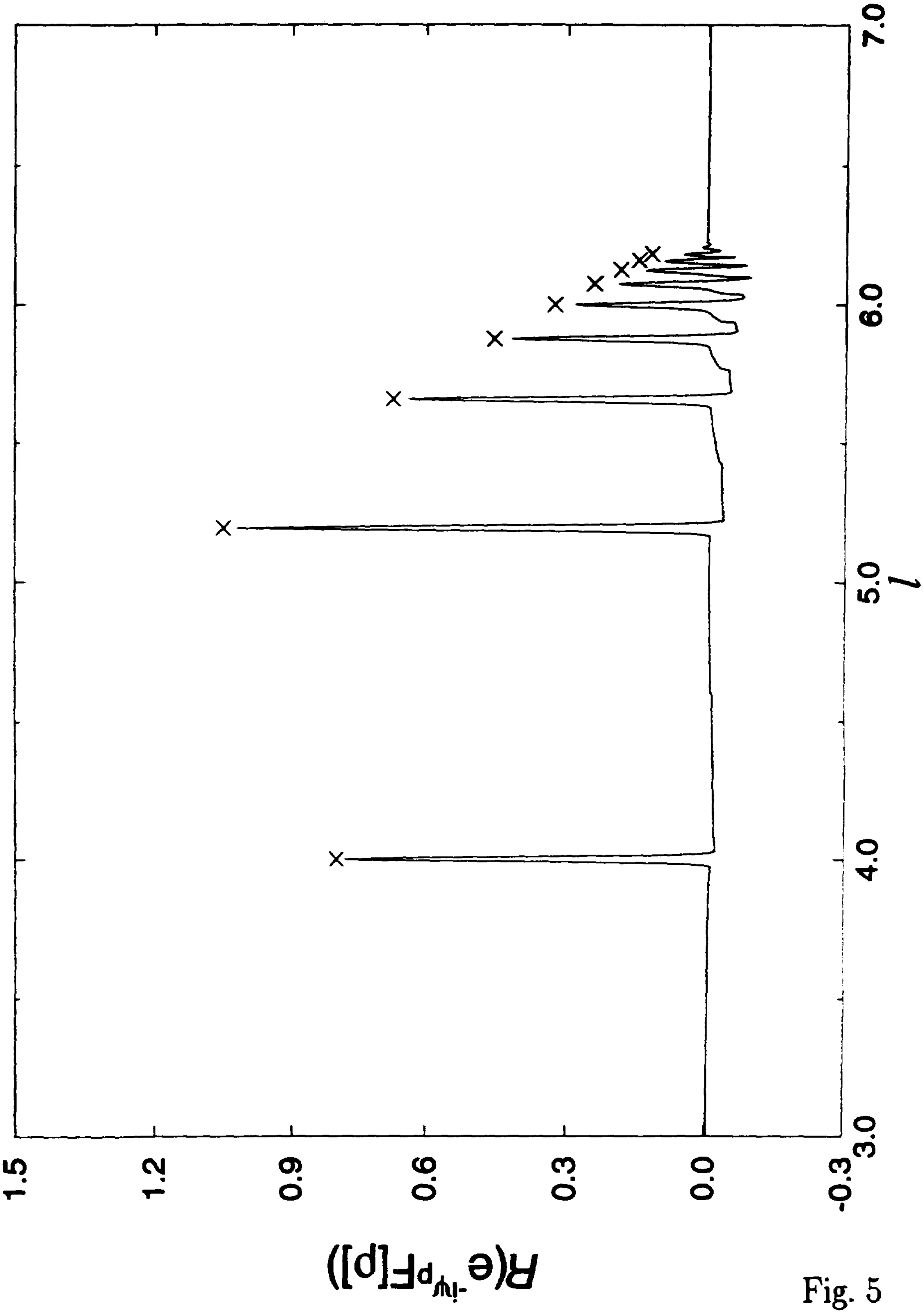

Fig. 5

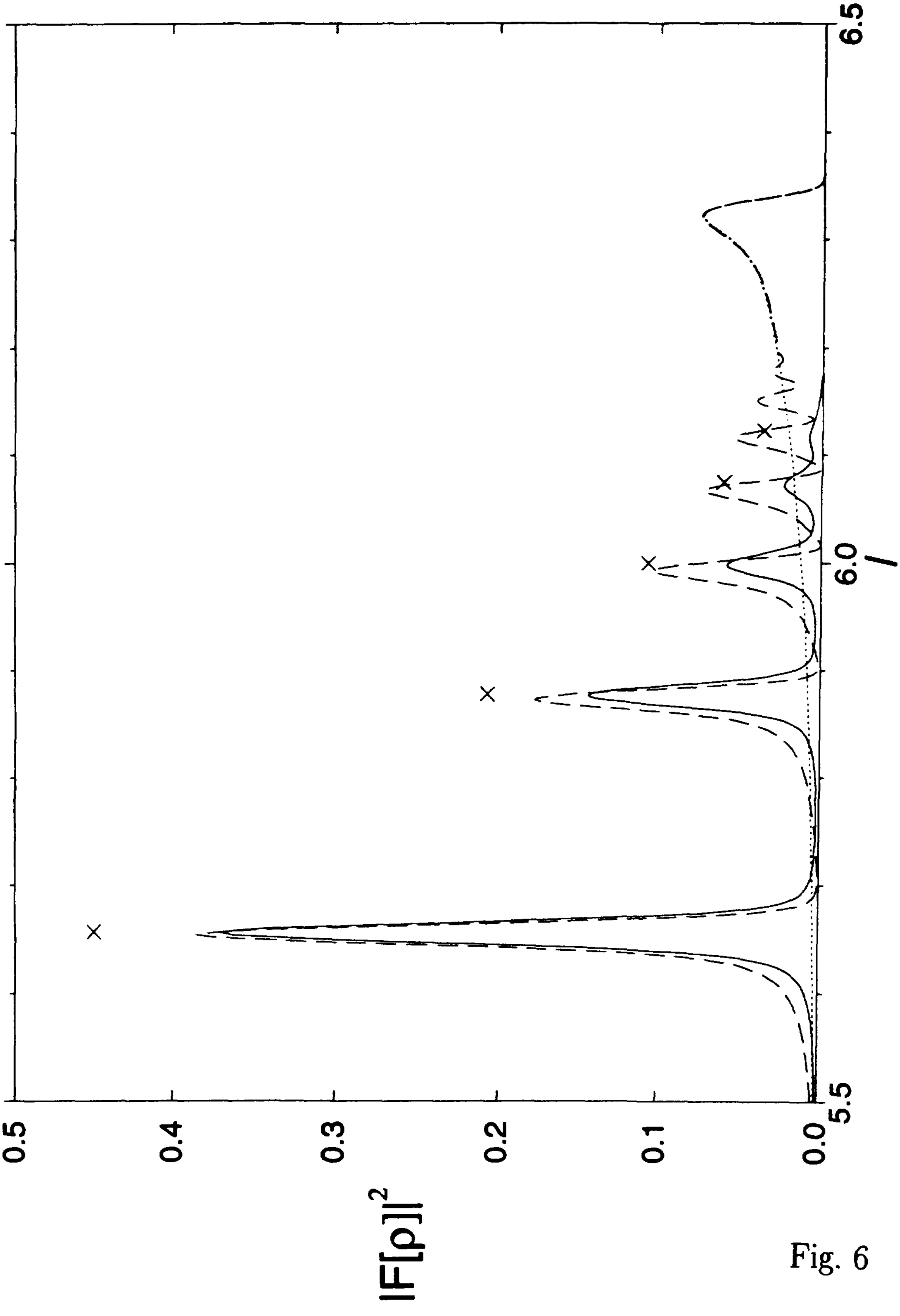

Fig. 6

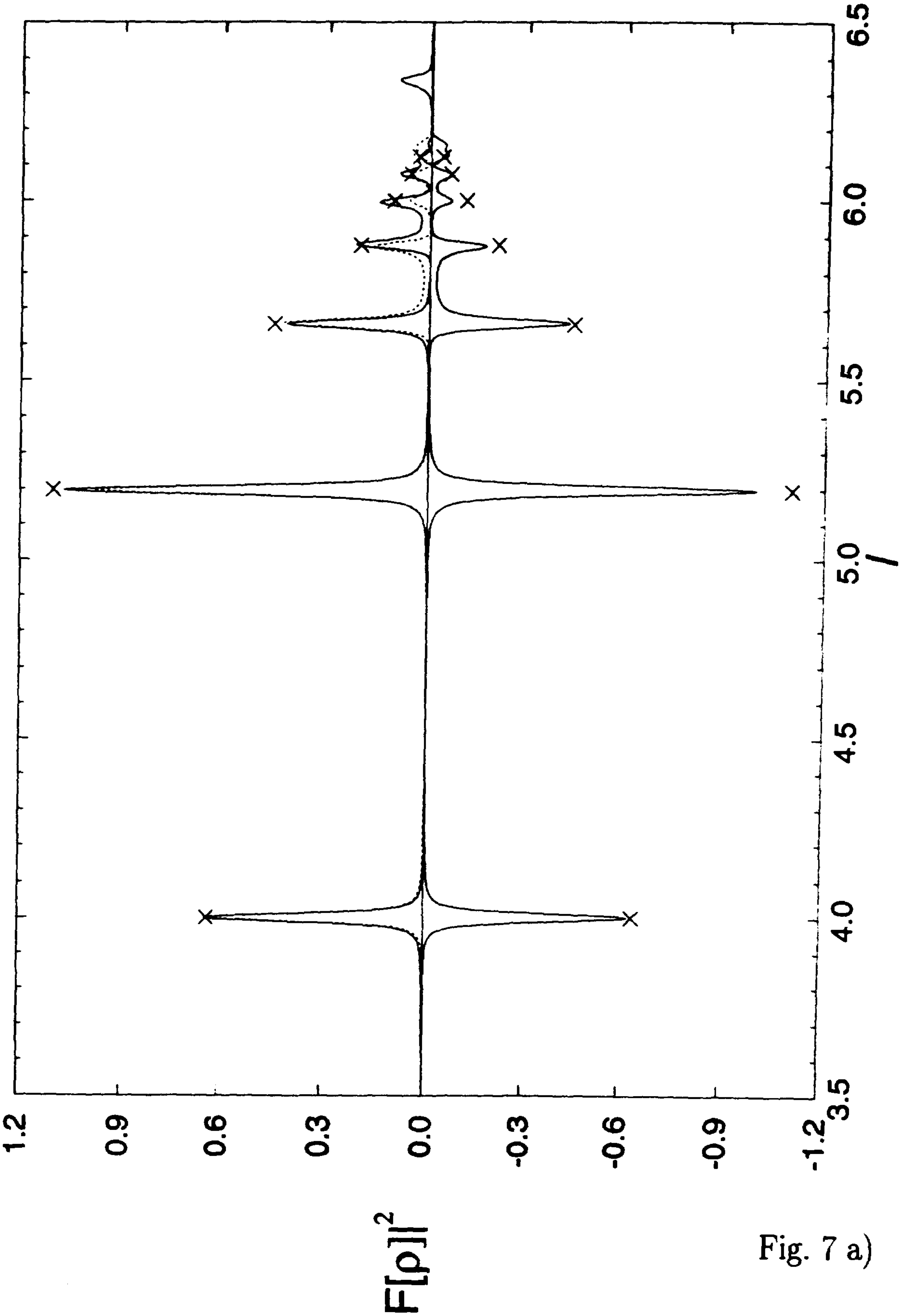

Fig. 7 a)

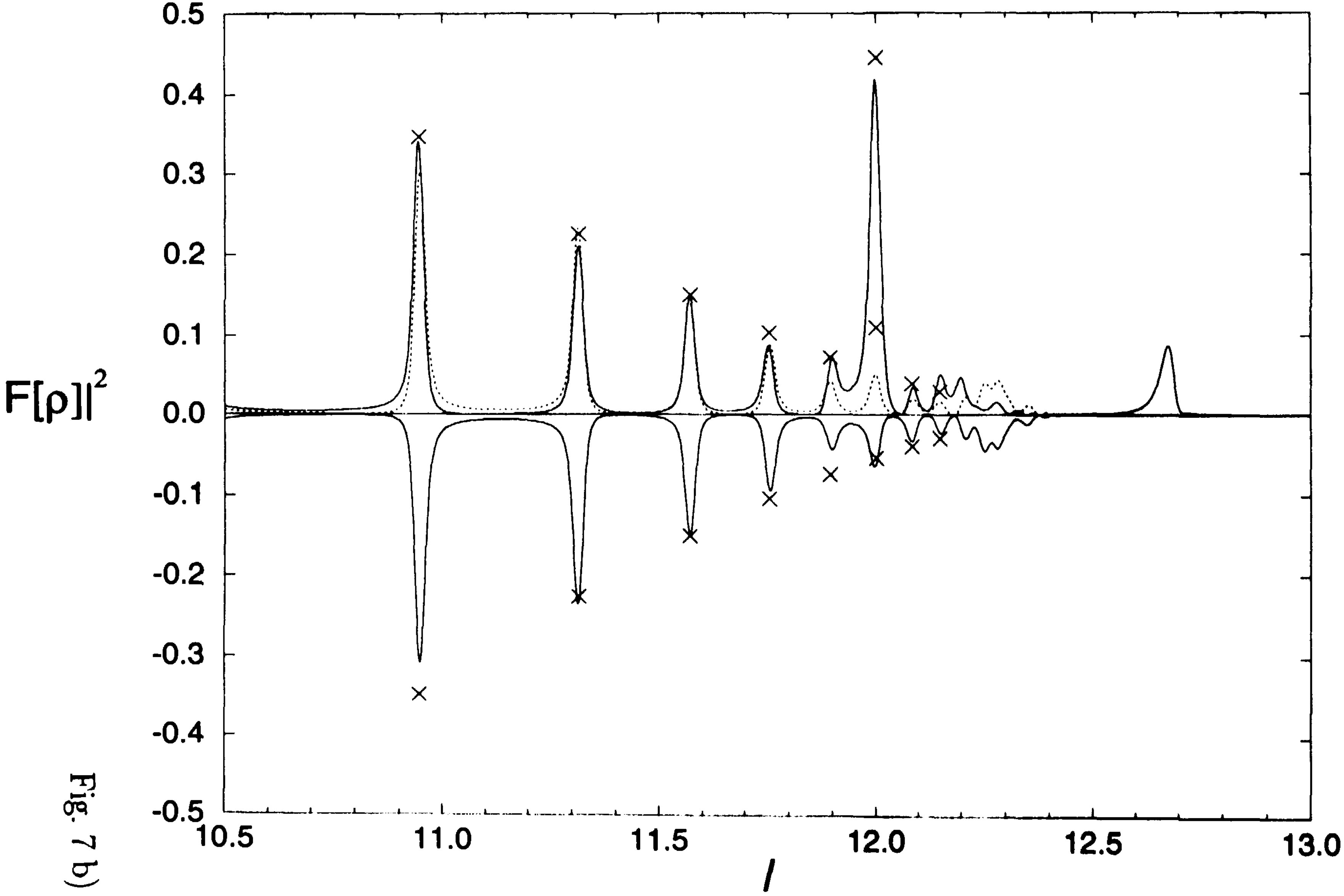

Fig. 7 b)

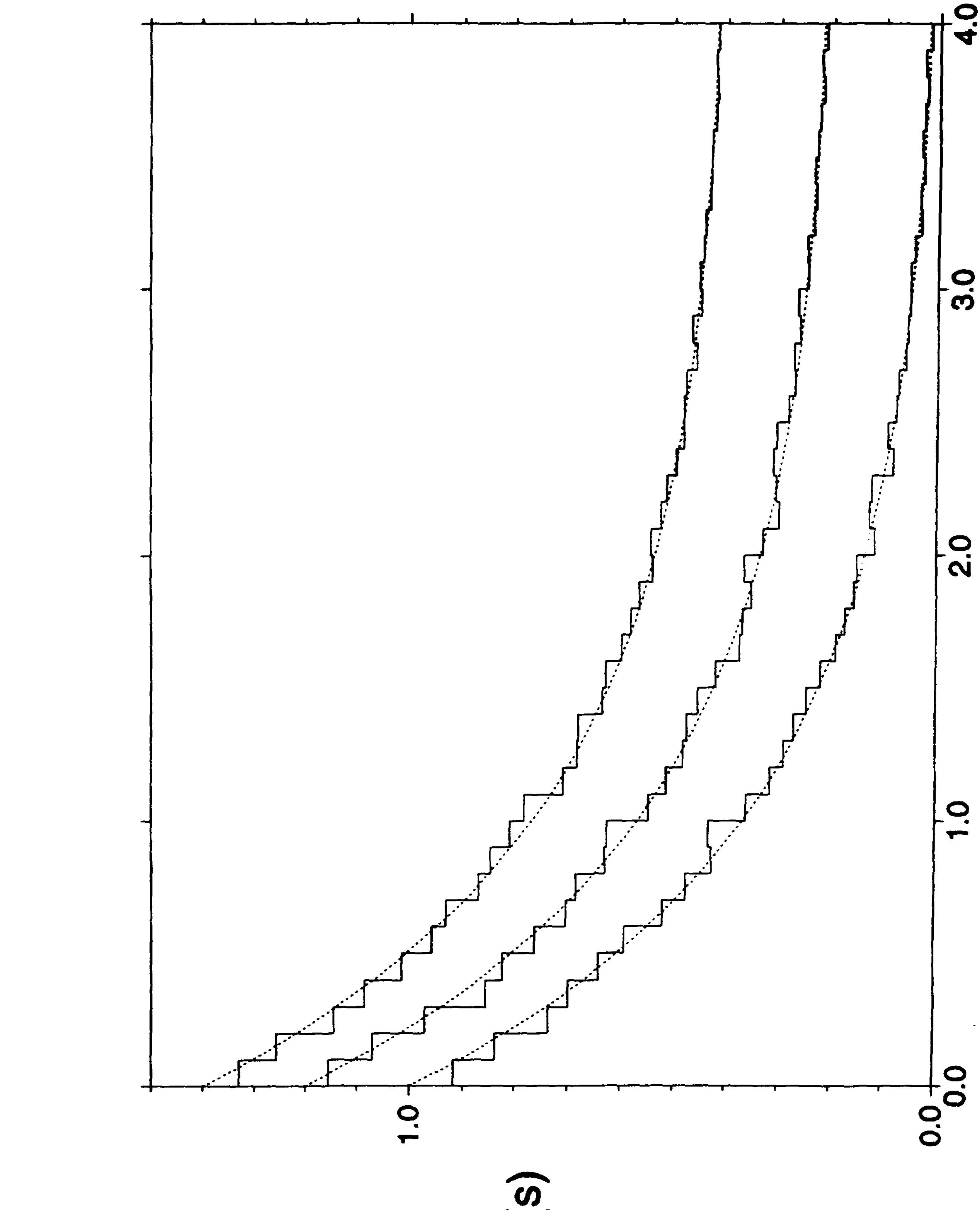

Fig. 8

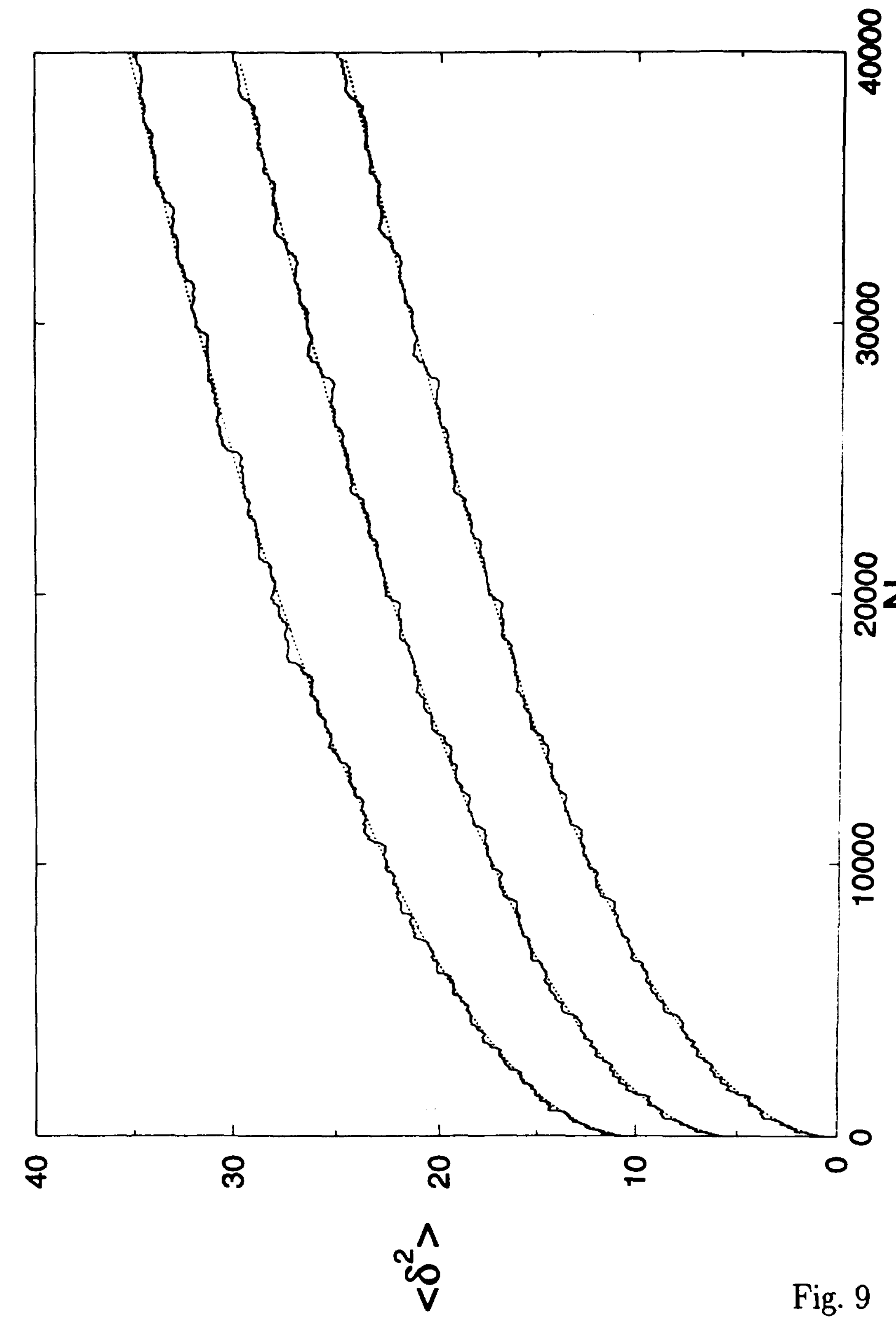

Fig. 9

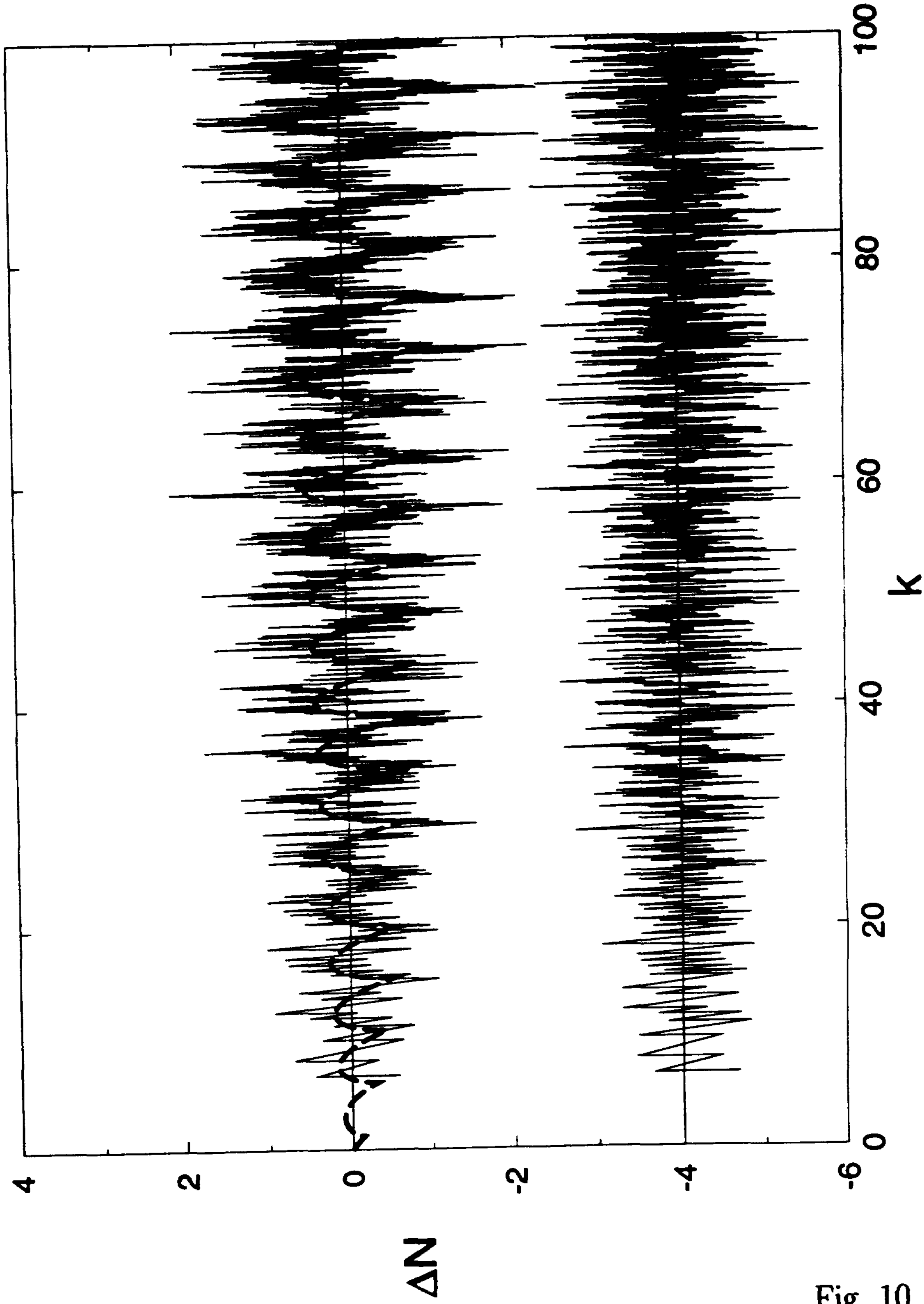

Fig. 10

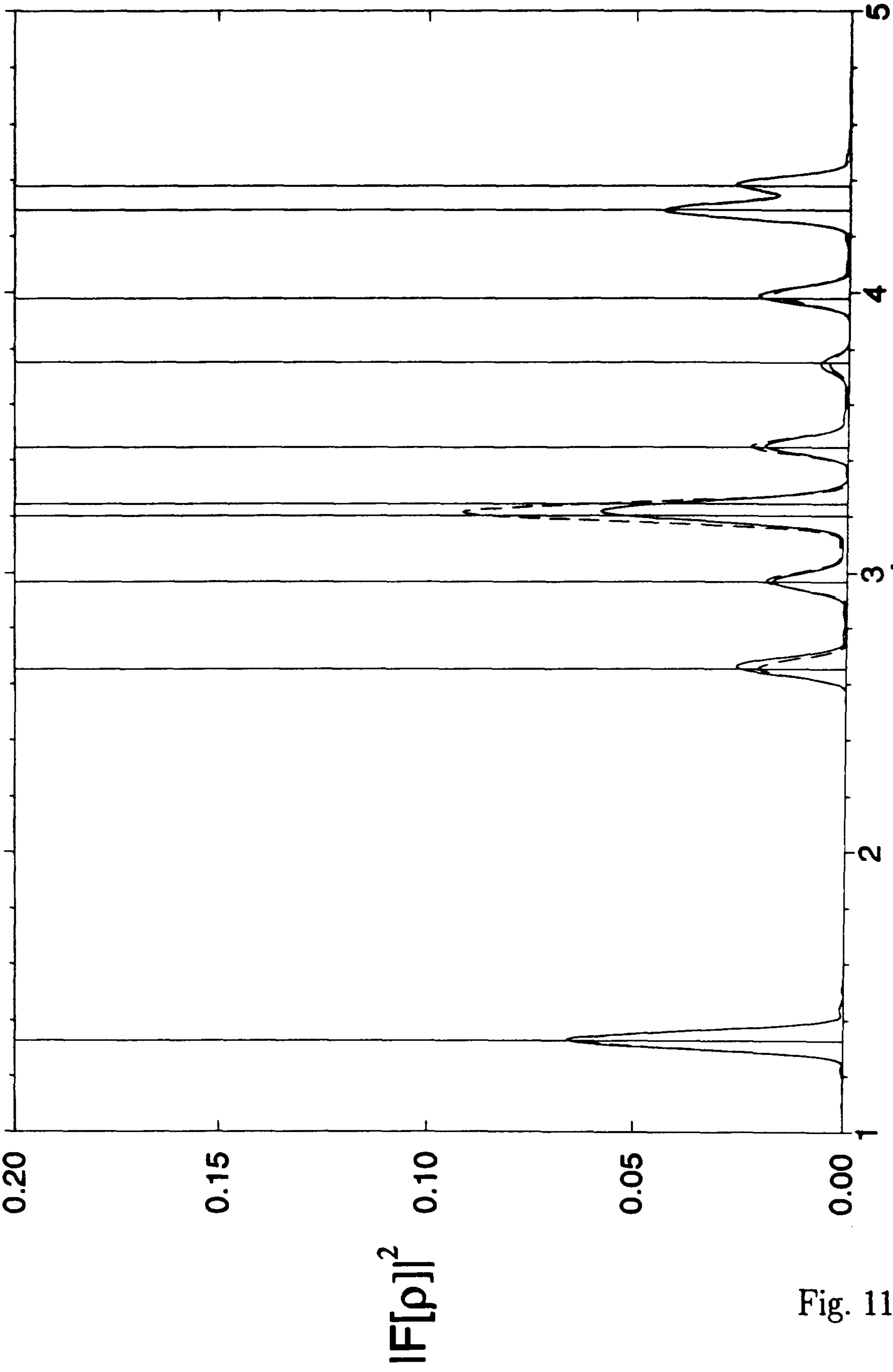

Fig. 11 a)

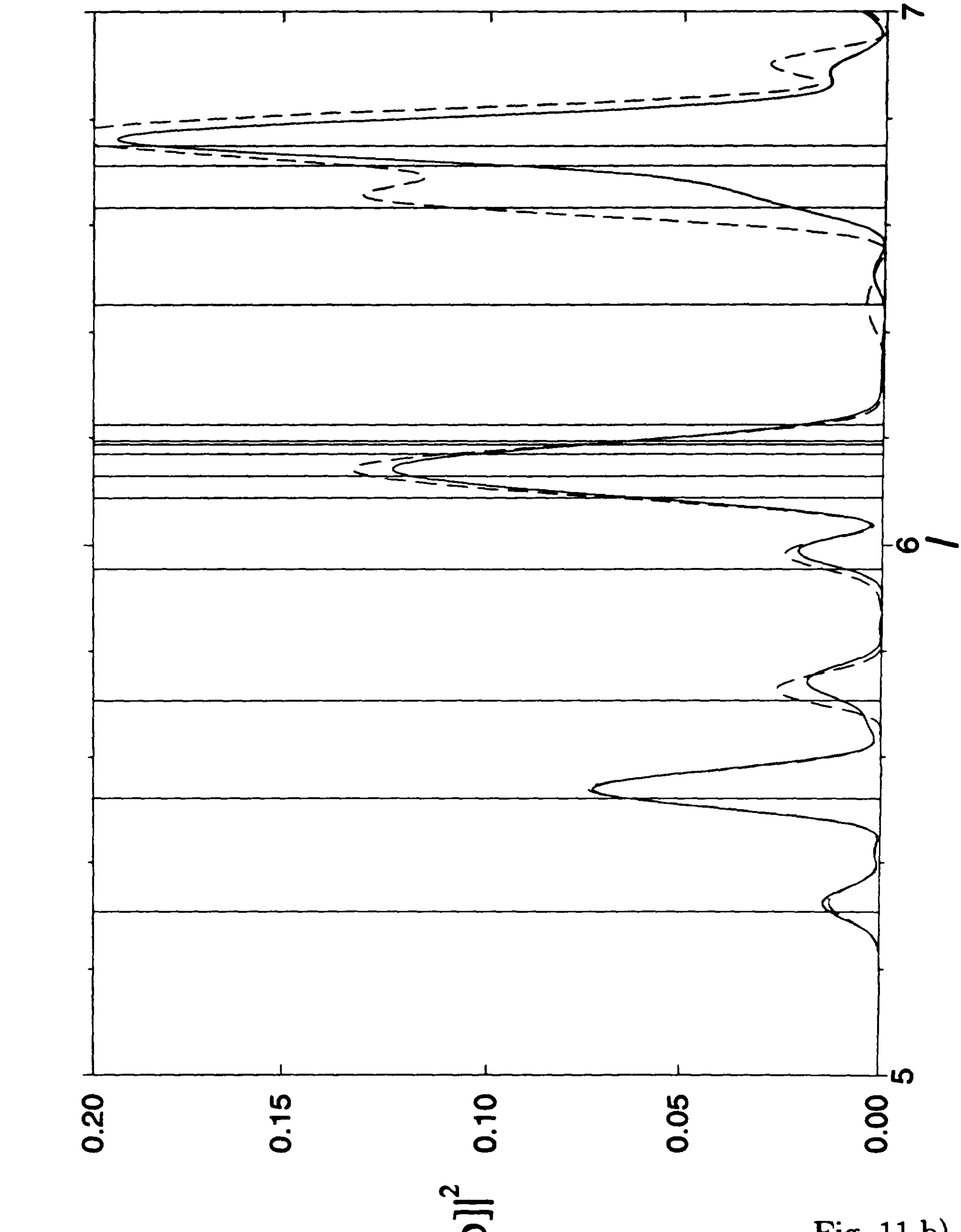

Fig. 11 b)

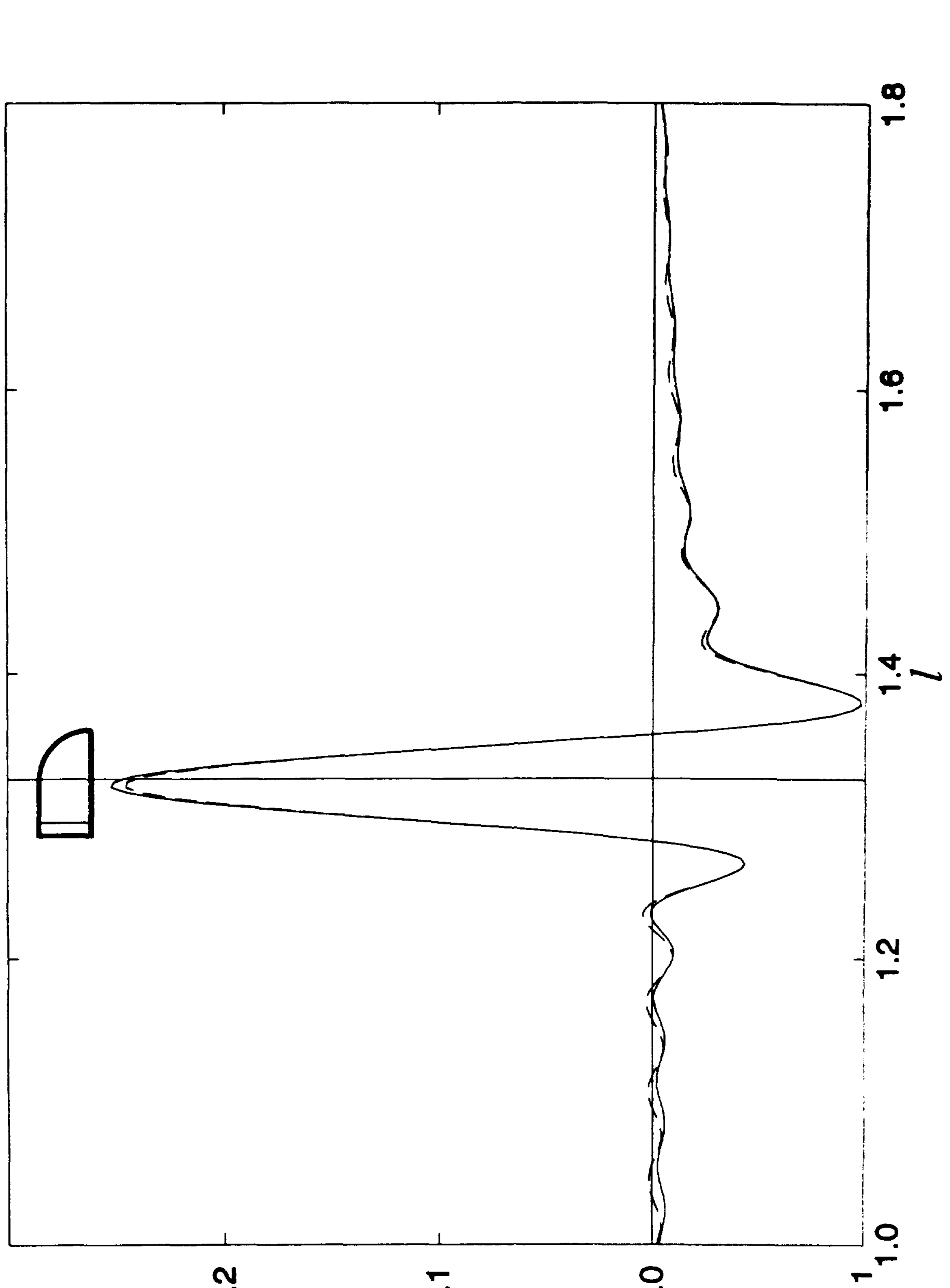

Fig. 12 a)

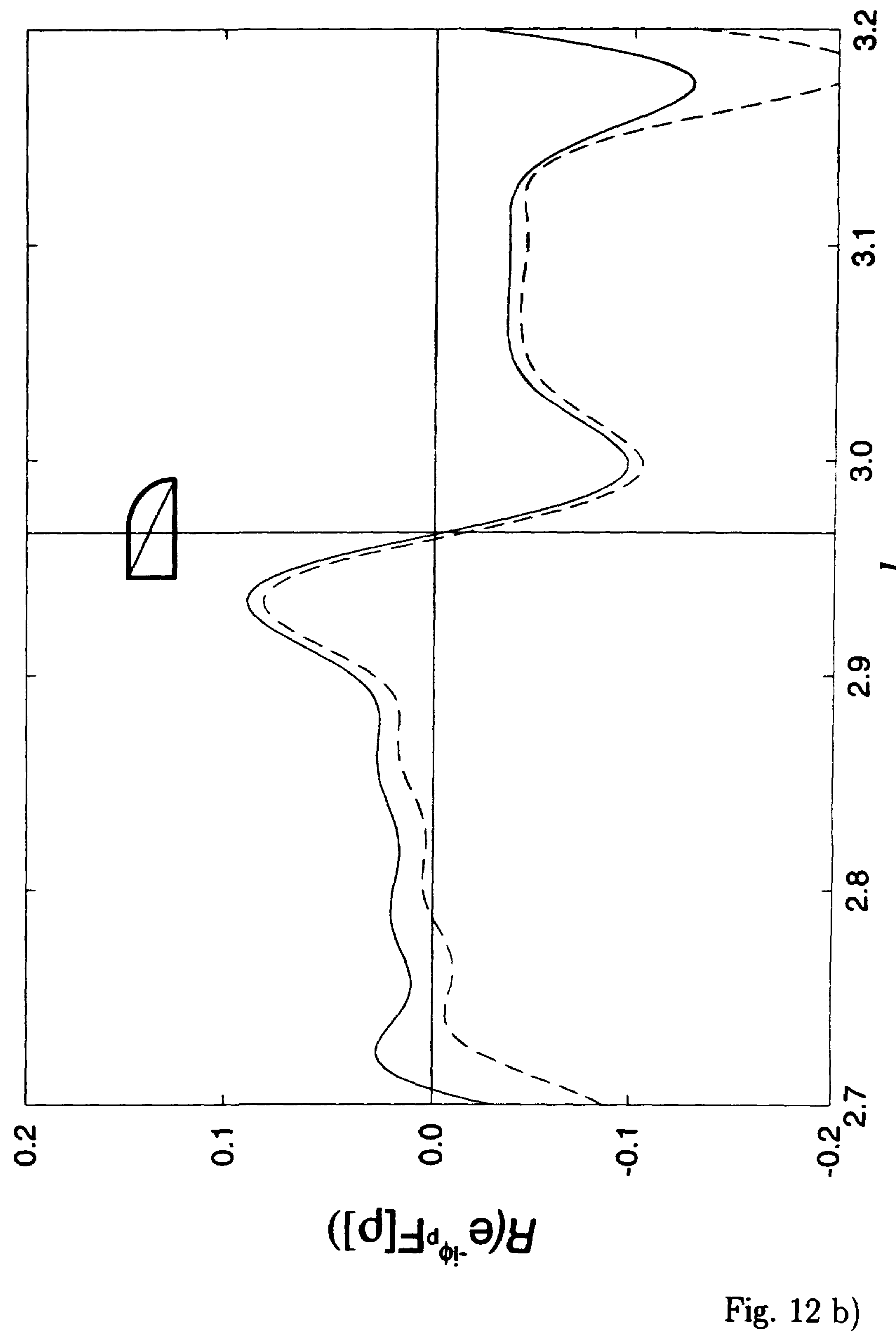

Fig. 12 b)

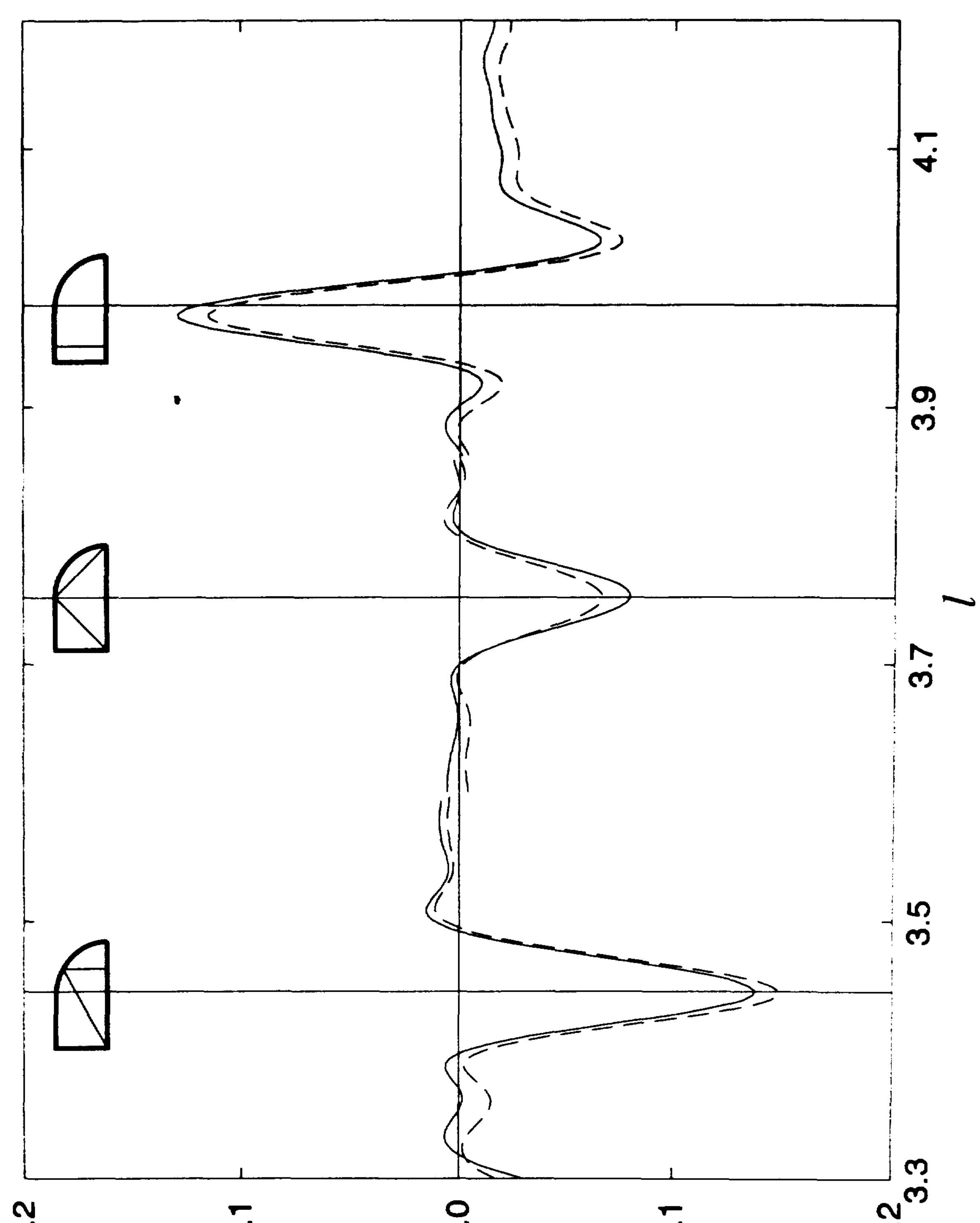

Fig. 12 c)

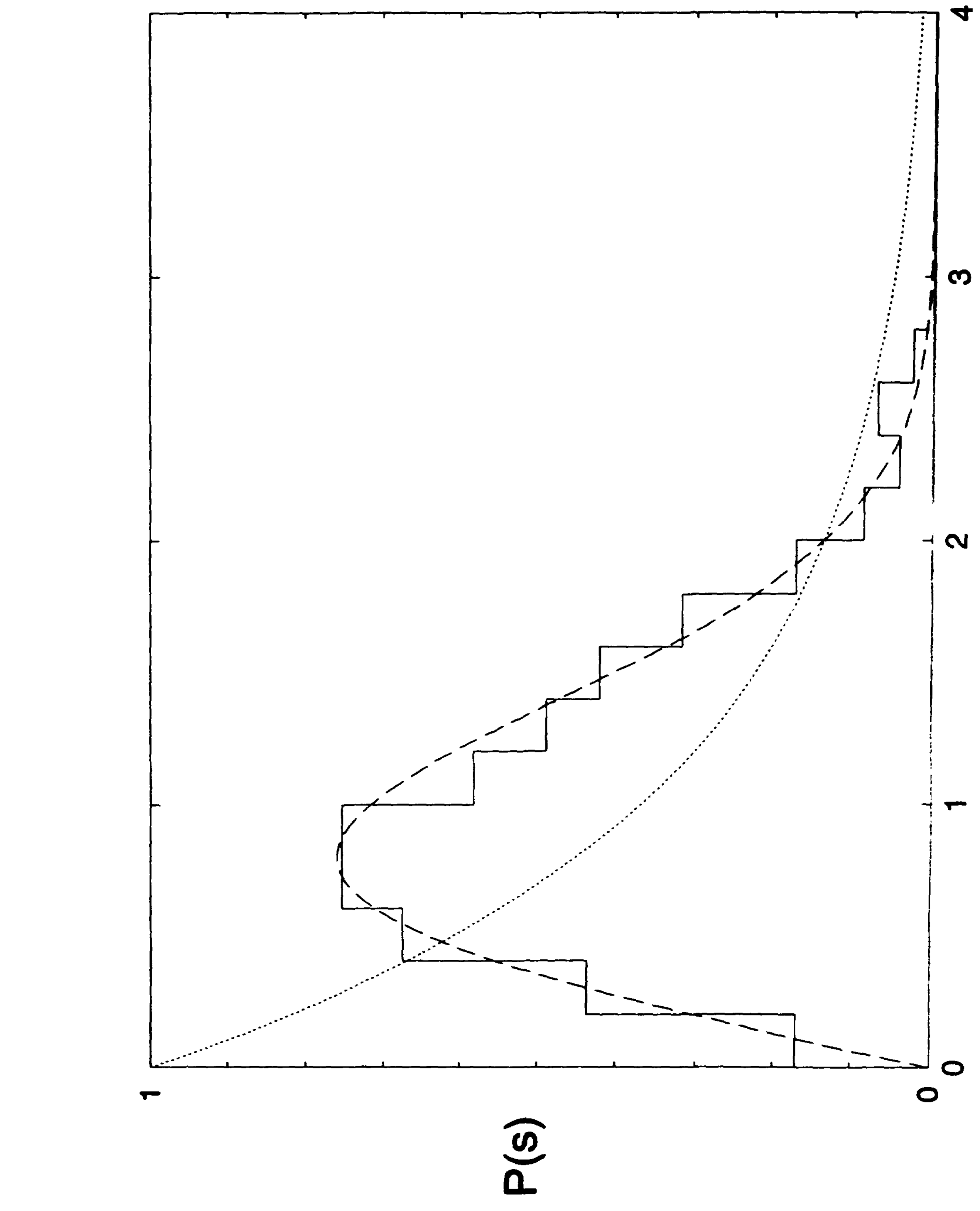

Fig. 13

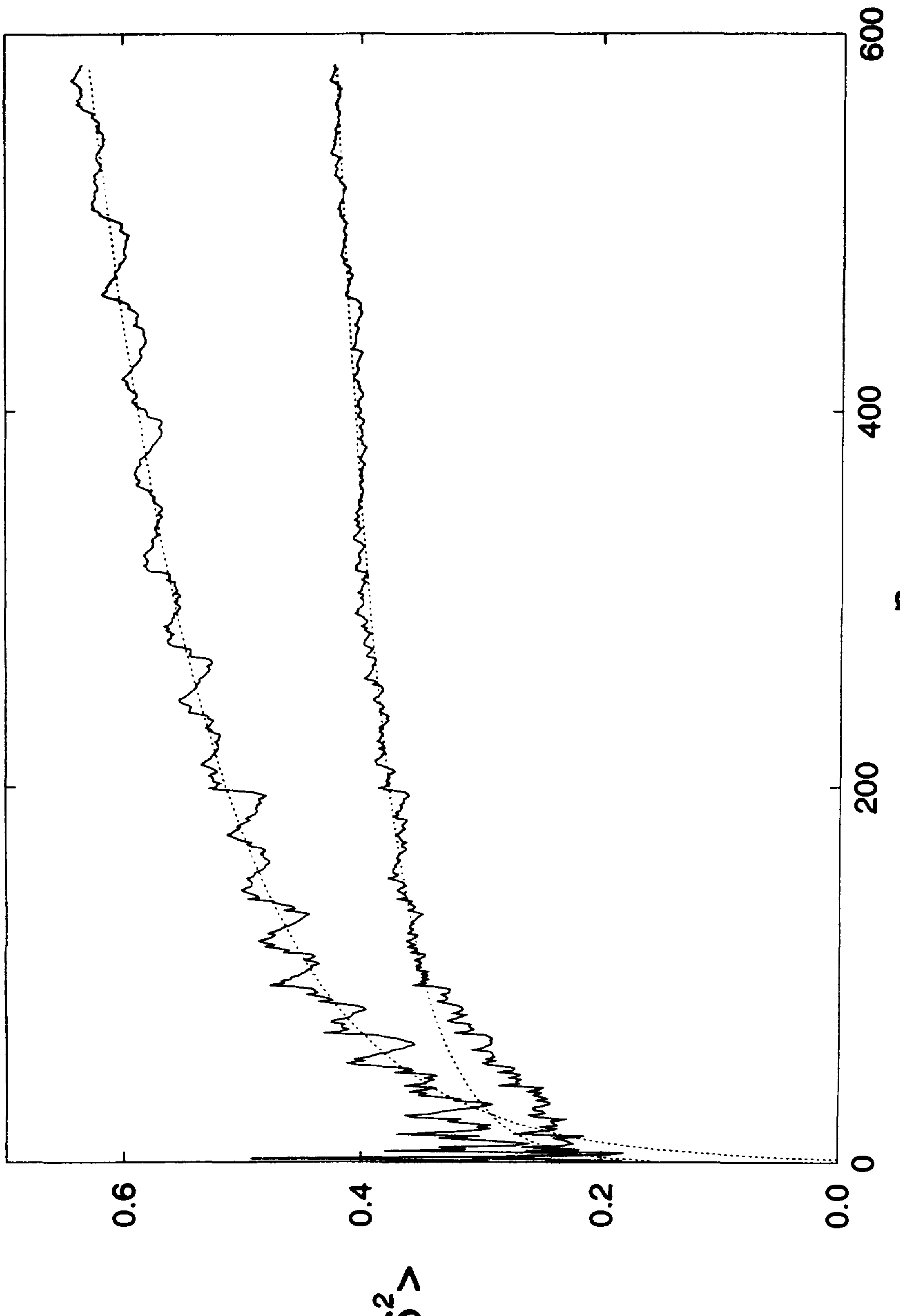

Fig. 14